

Confidential Disclosure Agreement Letter

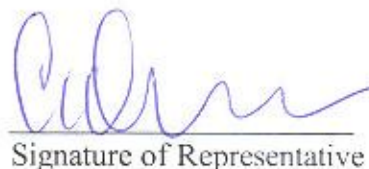
I, Markus Kolodzic, have disclosed herein certain confidential ideas and information regarding the chemical modification of surfaces and matrixes for biomolecule purification, which I refer to as my trade secrets. In partial fulfillment of my Diplom requirements, I have submitted a thesis, conducted under the guidance of Alpay Taralp, my Internship Supervisor, in which information relevant to my trade secrates have been incorporated, solely with the purpose and belief that you may more easily evaluate the scientific merit of my work and pass judgment on the concept of awarding a degree.

By reading the thesis subject matter hereafter, you agree to treat it as valuable proprietary trade secret information and maintain it in confidence. Accordingly, I have disclosed patentable aspects of this work with the understanding that you wish to have the opportunity to evaluate the subject matter as a whole on the following basis:

You agree not to disclose this confidential, proprietary, trade secret information to anyone other than those who reasonably need to know of it for purposes of assisting the evaluation process. Furthermore, you agree not to disclose these trade secrets to anyone outside of your organization and will not use this information for commercial purposes, except for your evaluation, unless you have the express written consent of Research and Graduate Policies, Sabanci University, or unless the trade secrets have already, or at any time in the future, become in the public domain or publicly disclosed by someone having a right to make such a public disclosure or information has been or is in the future disclosed to you by a third party who is lawfully in possession of the trade secrets and has a right to disclose them to you.

Sabanci University
Organization

Doc. Dr. Cemil Arkan
Organization Representative


Signature of Representative

05 / 03 / 2003
Date of Signature

Claims to Original Research

1. Mesoscale patterning of polymer surfaces was achieved by employing degradative chemical processes whose surface kinetics followed reaction-diffusion principles and operated under spatiotemporal control.
2. Pre-glass coatings along oxidized polypropylene surfaces were afforded, serving as a barrier material of the plastic and resisting the permeation of solvent.
3. Pre-glass coatings along oxidized polypropylene surfaces were afforded that reversibly adsorbed protein & mRNA and introduced the concept of developing a minimal-step, surface-mediated, tube-based purification format.
4. Low-surface-energy, non-adsorptive convenience plastics such as polypropylene tubes were conveniently aminated by oxidation of the surface, followed by activation, deposition and curing of amino moiety-bearing organosilane reagents.
5. Novel surfaces were rationally tailored directly onto plastic tubes and related convenience articles using the step-wise application of solution-phase reagents.
6. In changing the reaction-diffusion conditions of oxidation to afford correspondingly different mesoscopic surface topologies, the loading, non-covalent adsorption and retention of protein by oxidized polypropylene tubes was enhanced or weakened accordingly.

**MODIFICATION, CHARACTERIZATION, ANALYSIS AND
LIFE-SCIENCE APPLICATION OF POLYMERS:
POLYPROPYLENE**

Markus Kolodzie

A thesis submitted in partial fulfillment of the
requirements for the degree of

Diplomingenieur (Fachhochschule) der
Fachrichtung Chemie

Fachhochschule NTA,
Prof. Dr. Grüber, gemeinn. GmbH.,
88316 Isny im Allgäu

March 2003

© 2003 Markus Kolodzie, İstanbul, Turkey

Supervisor: Dr. Kurt Grillenberger

Internship-Supervisor: Dr. Alpay Taralp

This study was conducted at:

Faculty of Engineering and Natural Sciences,
Sabancı University, Istanbul

ACKNOWLEDGEMENTS

I would like to thank my internship supervisor Asst. Prof. Dr. Alpay Taralp of the Faculty of Engineering and Natural Sciences, Sabancı University, for providing me with guidance and advice throughout my one year internship and this study. Dr. Taralp always encouraged me and other students to benefit of all possibilities given to us by the university and by research. Therefore he spent as much of his free time with students in the laboratories as his young “family” allowed – and more. I also want to thank Dr. Taralp’s family for integrating me like a family member, which certainly gave me hope during hard times. I feel extremely proud, appreciative and privileged to have worked together with him and would be very pleased to work with him in the future again. It was always inspiring to work with a scientist and friend of his quality.

I would like also to thank my supervisor Dr. Kurt Grillenberger, Dr. Gerald Grübler, and the administrative staff of the Fachhochschule und Berufskolleg NTA, Prof. Dr. Grübler GmbH, Isny and Sabancı University for giving me the opportunity to fulfill my internship at the Faculty of Engineering and Natural Sciences of Sabancı University. This cooperation was a new experience for all parties and certainly not always easy to realize.

I am very grateful to all faculty, students and staff of the Faculty of Engineering and Natural Sciences, Sabancı University, for accepting me as a full member of their team and supporting my work and ideas. In particular, I want to thank Prof. Dr. Yuda Yürüm, Asst. Prof. Dr. Mehmet Ali Gülgün, Assoc. Prof. Dr. Yusuf Menceloglu and Assoc. Prof. Dr. Naci Inci for their support and interesting and inspiring teamwork.

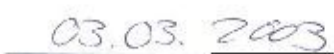
My labmates were always there to support, humor and stimulate. In particular, I want to thank my better half, Gözde İpek Özturk, for her smile, her support and filling my life with joy. I wish to thank also my friends Istem Özgen, Kazim Acatay, Çınar Öncel and Umut Soydaner for their friendship and time they spent with me.

Last but not least, I want to thank my family for their incessant and considerable support throughout my internship, and indeed, throughout my life.

Herewith I confirm, that this thesis was written by me, without accepting unlawful help
from others:



Name



Date

ABSTRACT

Three stepwise chemical approaches were developed to transform commercially available isotactic polypropylene tubes into specialty plastics for application in the life sciences:

Oxidation. Ordinary polypropylene surfaces were oxidatively transformed into high-surface plastics bearing reactive surface groups by reaction with aqueous persulfate. Attenuated-Total-Reflectance (ATR) infrared spectroscopic analysis indicated that ketone, carboxylic acid and hydroxyl groups were afforded within the plastic. Surface analyses using optical microscopy revealed the formation of macroscopic parallel cracks. More importantly, scanning electron microscopy indicated the reacted material had developed a mesoscopic topology remarkably similar in appearance to microvilli. Protein immobilization experiments conducted using fluorescently labeled albumin served to quantify the performance of oxidized surfaces. Facile detection by visual observation under UV light disclosed that adsorbed protein was released during sequential washings of the tubes in high salt, low salt and detergent solutions.

TEOS deposition. Hydrolysis products of tetraethoxysilane were cured onto oxidized, high-surface polypropylenes, affording tubes coated with pre-glass layers on the walls. ATR infrared spectroscopic analyses verified the glass-like end product. These modified surfaces possessed the appropriate physico-chemical traits to reversibly bind mRNA, thus establishing the concept of a tube-mediated approach to purify mRNA out of total RNA. Protein could also be reversibly bound to the surface

Triaminopropylsilane deposition. Oxidized surfaces were transformed using the hydrolysis products of trimethoxysilylpropylideneetriamine to afford functional surfaces bearing surface-pendent amino groups. ATR infrared spectroscopy revealed that the network formed by triaminopropylsilyl moieties described a thin coating upon the surface. Ninhydrin colorimetric analyses indicated that the surface amino group loading per unit frontal area had increased by an order of magnitude in comparison to commercially aminated surfaces. As in the case of the TEOS tubes, the amino-modified tubes adsorbed protein reversibly. The amino moieties were subsequently transformed with glutaraldehyde solutions to afford surface-bound aldehyde functional groups. This time, immobilization studies using fluorescent albumin indicated that protein retention was remarkably resistant to washings with high salt, low salt and detergent solutions. In comparison to the aldehyde surfaces, native surfaces did not retain protein to any significant degree, and oxidized, TEOS, and triaminopropylsilylated surfaces showed merit in applications based upon a reversible association. Protein binding and retention was markedly influenced by mesoscale topology in the absence of covalent surface-protein interactions.

TABLE OF CONTENTS

	Page No:
Confidential Disclosure Agreement Letter	i
Claims to Original Research and Publications Arising From This Thesis	ii
Acknowledgments	v
Abstract	vii
Chapters	
1. Introduction	7
1.1. Definition and History of Polymers	7
1.2. Importance of polymers	9
1.3. Properties of Polypropylene	11
1.4. Production of Polypropylene	13
1.4.1. Polymerization	13
1.4.2. Processing	14
Extruding	
Injection Molding	
1.5. Modification of Polypropylene	17
1.5.1. Modification Methods During Polymerization and Processing	17
Copolymerization	
Crosslinking	
Additives	
1.5.2. Modification Methods After Processing	19
Plasma Modifications	
Corona Discharge	
Flame Modifications	
1.6. Novel Modifications of Polypropylene	24

1.7.	References	25
2.	First Generation Surface: Oxidation of Polypropylene using Persulfate	26
2.1.	Introduction	26
2.2.	Material and Methods	27
Tubes, Chemicals and Proteins		
2.2.1.	General Methods (GM):	27
(i)	Preparation of Persulfate and Control Solutions	
(ii)	Reaction Method	
(iii)	Washing and Drying Method for Modified Eppendorf Tubes	
(iv)	Preparation and ATR-FTIR Analysis of Eppendorf Tubes	
(v)	Preparation and Optical Microscope Characterization of Tubes	
(vi)	Preparation and Scanning Electron Microscopy (SEM)	
(vii)	Trace Dansylation of Bovine Serum Albumin (BSA)	
(viii)	Immobilization Methods for Trace Dansylated Protein UV-Analyses	
2.2.2.	Analyses of Starting Polymer: Eppendorf Safe-Lock Tubes	32
(i)	Scanning Electron Microscopic (SEM) Analysis of Native Surfaces	
(ii)	X-ray Powder Diffraction Analysis of Native Eppendorf Tubes	
(iii)	Differential Scanning Calorimetry (DSC) of Native Eppendorf Tubes	
(iv)	ATR-FTIR Analysis of Native Eppendorf Tubes	
2.2.3.	Oxidation experiments:	33
(i)	Concentration Course	
(ii)	Time Course	
(iii)	Oxidation of Tubes under Static Conditions	
(iv)	Oxidation of Tubes in a Rotating Speedvac Concentrator	
(v)	Oxidation of Tubes in a Rotating Thermomixer	

2.3.	Results and Discussion	38
(i)	Analysis of Native Eppendorf Tubes	
(ii)	Concentration Course	
(iii)	Time Course	
(iv)	The Nature of Oxidation Reactions	
(v)	Extent of Penetration of Oxidation	
(vi)	Microscopic Analyses	
(vii)	Protein Immobilization	
2.4.	Conclusions	60
2.5.	Acknowledgements	60
2.6.	References	61

3. Second Generation Surface: Coating of Oxidized Surfaces using TEOS	64
3.1. Introduction	64
3.2. Materials and Methods	66
Silanes, Chemicals, Proteins and Kits	
3.2.1. General Methods (GM):	66
(i) Preparation of Silane Solutions	
(ii) Washing and Drying of Coated Surfaces	
(iii) Preparation and ATR-FTIR Analyses of Eppendorf Tubes	
(iv) Trace Dansylation of Bovine Serum Albumin (BSA)	
(v) Immobilization Method for Trace Dansylated Protein UV-analyses	
3.2.2. Second Generation TEOS Coating Procedure	68
3.2.3. Life-Science Application of TEOS-Coated Surfaces: mRNA Purification	69
(i) Preparation of Oxidized Surfaces for mRNA Purification	
(ii) TEOS Coating Procedures for mRNA Purification	
(iii) Isolation of Total RNA	
(iv) mRNA Isolation from Total RNA	
(v) Amplification and Analysis of Purified mRNA	
3.3. Results and Discussion	73
(i) TEOS Coating	
(ii) Protein Immobilization	
(iii) mRNA Purification	
3.4. Conclusion	79
3.5. Acknowledgements	80
3.6. References	81

4. Second Generation Surfaces: Oxidized Polypropylene coated using TMPDT	
4.1. Introduction	82
4.2. Materials and Methods	83
Silanes, Chemicals, Proteins	
4.2.1. General Methods (GM)	83
(i) Preparation of Aminosilane Solutions	
(ii) Washing and Drying of the Coated Surfaces	
(iii) Preparation and Ninhydrin Analyses of Coated Surfaces	
(iv) Preparation and Glutaraldehyde Analyses of Coated Surfaces	
(v) Preparation and ATR-FTIR Analyses of Eppendorf Tubes	
(vi) Trace Dansylation of Bovine Serum Albumin (BSA)	
(vii) Immobilization Method for Trace Dansylated Protein Analyses	
4.2.2. Second Generation TMPDT Coating Procedure	86
4.3. Results and Discussion	87
(i) TMPDT Coating	
(ii) Glutaraldehyde Crosslinking	
(iii) Protein Immobilization	
4.4. Conclusion	95
4.5. Acknowledgements	96
4.6. References	96
General conclusion	97

APPENDIX

I. Specifications of Analytical Equipment	98
(i) Attenuated Total Reflectance Infrared Spectrometer (FT)	
(ii) X-Ray Powder Diffractometer	
(iii) Differential Scanning Calorimeter (DSC)	
II. Resume	100

Chapter 1: Introduction

1.1 Definition and History of Polymers

The word *polymer* is a combination of the classical Greek words *poly* meaning “many” and *mere* meaning “parts”. Simply put, a polymer is a long-chain molecule that is composed of a large number of identical repeating units. Certain polymers can be found in nature, such as proteins, cellulose and silk, while many others are produced by synthetic routes. In modern times many naturally occurring polymers are also produced synthetically as the demand of industry is so great that nature itself cannot fully supply these polymers.

Different polymers feature their own unique set of properties. Polymers capable of high extension under ambient conditions find important applications as elastomers, like nitrile or butyl rubber. On the other hand, polymers which afford characteristics that permit their formation into long fibers are suitable for textile applications, such as nylon and polyesters.

In contrast to the usage of the word *polymer*, those commercial materials, other than elastomers and fibers, that originate from synthetic polymers are called *plastics*. Typical commercial plastic resins contain usually two or more polymers and additives, which are used to improve specific properties of the final product [1].

The birth of polymer science can be followed back to the mid-nineteenth century, to a scientist named Charles Goodyear. Goodyear developed in the 1830's the vulcanization process that transformed the sticky latex of natural rubber into a useful elastomer which formed the basis of the famous Goodyear™ tire company. Later in the 1860's Christian F. Schönbein synthesized the first man-made thermoplastic, namely, celluloid. In 1907 Leo Baekeland synthesized a phenol-formaldehyde resin known as Bakelite as well as an unsaturated polyester resin known as Glyptal. Both of his polymers were later used as protective coatings by General Electric. Until 1940 several polymeric compounds were synthesized by companies like Du Pont, Dow and ICI including important examples like

nylon, Teflon™ and polyethylene. Also polymers like polystyrene were produced in ton-scale for the first time [1]. World War II forced American and British scientists to develop new polymeric materials like synthetic rubber, as Asian allies cut the supply of many naturally occurring materials like the Hevea rubber, better known as natural rubber [2]. In the 1950's polymer production was revolutionized by the introduction of new polymerization catalysts by Ziegler and Natta. These new polymerization methods using stereospecific transition-metal catalysts afforded led the commercialization of polypropylene as a major commodity plastic. In the 1960's and 1970's a number of high-performance polymers was developed which competed favorably with more traditional materials, such as metals, for automotive and aerospace applications [1].

1.2 Importance of Polymers

Today, polymeric materials are used in nearly all areas of daily life. One of the most common polymers is polyethylene (PE) and its related products LDPE, HDPE, LLDPE and UHW-HDPE are afforded by different polymerization methods and copolymerization. This polymer-family is generally applied to films, foils (LDPE, LLDPE), bottles, cans, cable isolation (HDPE) and high technology materials like artificial hip joints (UHW-HDPE). Another important polymer is polypropylene (PP) which is used in various applications like household gadgets, films, cans and bottle caps. A great benefit of polypropylene is also that it can be steam sterilized which introduces applications like medical packagings, disposable syringes and equipment for biochemical laboratories. Other important polymers are polystyrene (PS; disposable cups and cutlery) polyvinylchloride (PVC; pipes, cable isolation, floor carpeting) polymethylmethacrylate (PMMA; protective glass, casings) and polyetheneterephthalate (PET; fibers, films, food packing) [3].

The demand for polymers increased over the last years. Polymer production statistics show in particular that polypropylene (PP) is one of the polymers produced in highest amounts. Forecasts based on the production growth-rates between 1995 and 2002 indicate that the production of polypropylene will increase more than the production of other polymers in the next following 10 years [4].

The high demand placed on polypropylene can be explained by the fact that polypropylene has developed over the recent years as the dominant polymer of the appliance industry. This industry can be divided in three main parts. The household appliances, "white" goods and "brown" goods. Household appliances include 'smaller, general appliances which can be usually found in the kitchen, house and garden. Examples of this kind of appliances are parts of coffee machines or water boiling kettles. White goods include larger appliances used in households, like washing, cooking and refrigeration equipment. In this field many applications have been developed for internal components replacing polymers like PVC and metals. polypropylene used in other consumer electrical goods, such as home computers, belongs to the 'brown' goods. In these three appliance

fields polypropylene is usually used in modified versions to offer enhanced properties of temperature stability, processability and stiffness.

The laboratory-equipment industry describes another important part of the polypropylene market. polypropylene is used for various applications in research laboratories in modified as well as unmodified forms. Examples of polypropylene laboratory equipment include storage containers and racks, plastic beakers, reaction tubes, pipette tips, well-plates and selected parts of electrical laboratory equipment. Modification enhances the scope of applications for polypropylene, affording for example, fire hazard, anticorrosion, reinforced or microporous polypropylene [5]. These facts indicate that polypropylene is one of the most important polymers used in daily life.

1.3 Properties of Polypropylene

Polypropylene can be used in various applications because of its good mechanical, thermal, physical and processing properties. Two noteworthy properties of polypropylene are the high impact strength and the good fatigue endurance (table 1).

Mechanical Properties	Conditions		
	State 1	State 2	ASTM
Elastic Modulus (MPa)	897 - 1242	Tensile	D638
Flexural Modulus (MPa)	897 - 1380	23 °C	D790
	276	94 °C	D790
	207	122 °C	D790
Tensile Strength (MPa)	21 - 30	at yield	D638
	28 - 38	at break	D638
Compressive Strength (MPa) at yield or break	25 - 56		D695
Flexural Strength (MPa) at yield or break	35 - 49		D790
Elongation at break (%)	200 - 500		D638
Hardness	65 - 96	Rockwell R	D638
	70 - 73	Shore D	D638
Izod Impact (J/cm of notch) 1/8" thick specimen unless noted	0.6 - 7.4		D256A

Table 1: Mechanical properties of polypropylene [6].

The most important thermal properties of polypropylene are high heat resistance and low thermal conductivity (table 2).

Thermal Properties	Conditions		
	Pressure	State	ASTM
Coef of Thermal Expansion ($10^{-6}/^{\circ}\text{C}$)	68 - 95		D696
Deflection Temperature ($^{\circ}\text{C}$)	85 - 105	0.46 MPa	D648
	55 - 60	1.82 MPa	D648
Thermal Conductivity (W/m- $^{\circ}\text{C}$)	0.146 - 0.167		C177

Table 2: Thermal properties of polypropylene [6].

Polypropylene is a convenient plastic for processing, as it displays a sharply-defined melting point, high shrinkage after molding and the ability to flow in thin-walled sections (table 3).

Processing Properties		Conditions	
		Type	ASTM
Melt Flow (gm/10 min)	0.6 - 100		D1238
Melting Temperature (°C)	-20	T _g , amorphous	
Melting Temperature (°C)	150 - 175	T _m , crystalline	
Processing Temperature (°C)	191 - 288	Injection molding	
	205 - 260	Extrusion	
Molding Pressure (MPa)	69 - 138		
Compression Ratio	2 - 2.4		
Linear Mold Shrinkage (cm/cm)	0.01 - 0.025		D955

Table 3: Processing properties of polypropylene [6].

Additional favorable properties of polypropylene are its high chemical resistance and low water absorbtivity (table 4).

Physical & Electrical Properties		Conditions	
		State	ASTM
Specific Gravity	0.89 - 0.905		D792
Water Absorption (% weight increase)	0.03	After 24 hrs	D570
Dielectric Strength (V/mil); 1/8" thick specimen unless noted	600		D149

Table 4: Physical and electrical properties of polypropylene [6].

These properties suggest that polypropylene is a suitable polymer for various applications of wide scope from construction products to high-technology functionalized, bioactive plastics.

1.4 Production of Polypropylene

1.4.1 Polymerization

Like most commercially produced unmodified polymers, polypropylene products are produced in two steps. In the first step the polymer is polymerized out of its monomers affording polymer granules. In the second step these granules are processed into their final application form by twin screw extruding, injection molding or calendering methods.

The polymerization of propylene is normally carried out in the presence of a catalyst of the Ziegler-Natta-type. Under appropriate conditions, polymer of a certain molecular weight and narrow size distribution can be made (Figure 1). Isotactic, atactic and syndiotactic format of polypropylene are known.

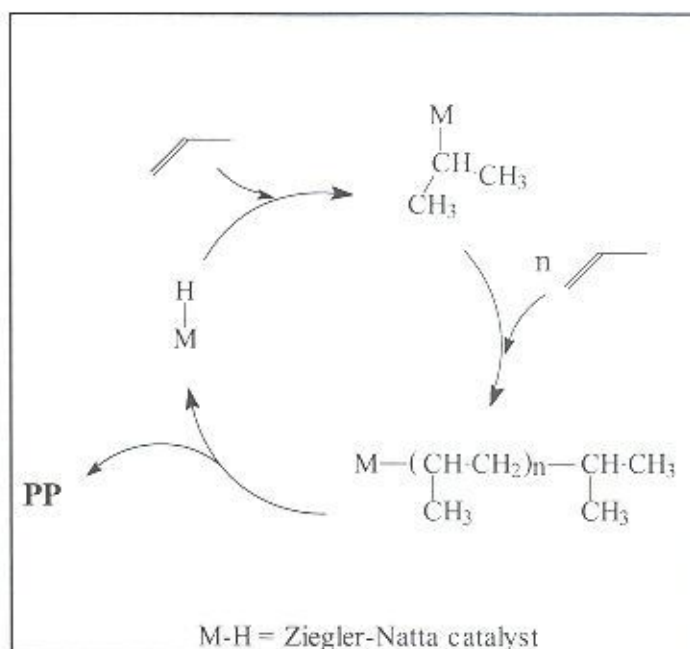


Figure 1: Polymerization mechanism using Ziegler-Natta catalysis.

Ziegler-Natta-type polymerization was introduced in 1954 by G. Natta, who modified the Ziegler-catalyst and revolutionized petrochemistry, introducing a catalyst that has since known as Ziegler-Natta catalyst. These catalysts consisted of $\delta\text{-TiCl}_3$ with

aluminum diethylchloride as activator. Over the next 20 years these catalysts were further refined resulting in the fourth generation of polymerization catalysts. The most significant advantage of the new generation catalysts was their high stereospecificity. This fact and the ease of the removal of the new catalysts simplified polymerization, as the washing-out step of the catalyst and the purification step of the polymer was eliminated [5].

Recently this fourth generation material as well as metallocene catalysts are being used in the polymerization of PP. Liquid or gaseous propylene or a solution in inert hydrocarbon diluent such as hexane is used. The production of polypropylene by inert hydrocarbon slurry processes decreased recently, as most modern plants have adopted bulk or gas polymerization processes. By far the most commonly used bulk PP-process is the Montell's 'Spheripol Process'. During the polymerization process, the liquid propylene is polymerized at temperatures of 60-80°C and pressures of 35-40bar. The most common gas phase polymerization process is the 'Amoco-Chisso' process. The benefit of this method is the good economics, as it is a continuous process [5].

1.4.2 Processing

The discussed polymerization methods afford polymer pellets, which are further processed by extruding or injection molding.

Extrusion is a typical method used to continuous products like pipes, sheets, films and coatings. In other words, the extruder (Figure 2) is in principle a melt or viscosity pump. During the twin screw extruding process, polymer material filled in a hopper, is melted and the melt is pumped using a twin screw system into a die, which forces the melted polymer into the final form. Different types of twin screw extruders are used in industry. These types differ usually in the rotating direction and orientation of the screws (Figure 3) [7].

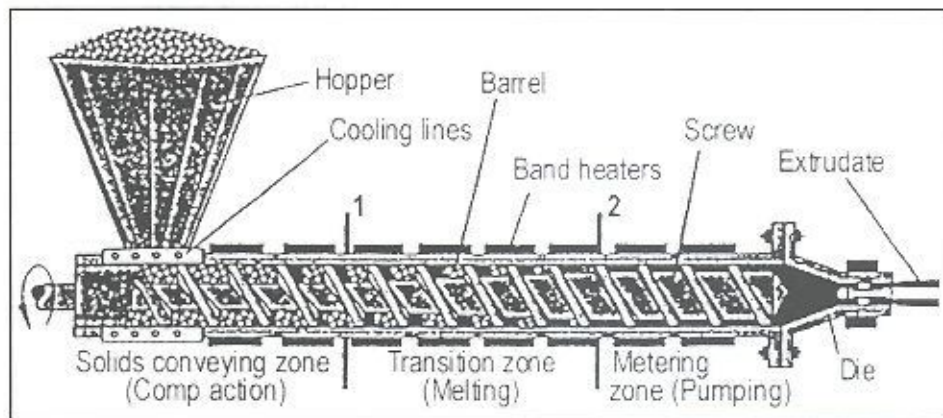


Figure 2: Schematics of an extruder.

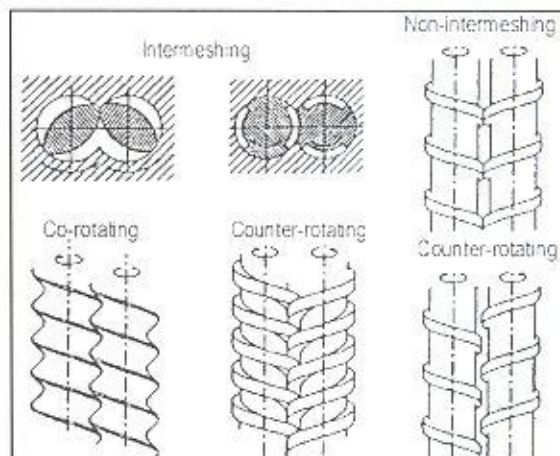


Figure 3: Different screw systems of extruders.

While extruding offers basically continuous products, injection molding is nowadays the most popular method to produce 3-dimensional products. Injection molding is a production method for large series and is almost not limited by factors of part shape or product size. The polymer melting and transport process is basically identically with the extruding process. Polymer is melted and transported by a screw system to the injection unit of the injection molding machine (Figure 4).

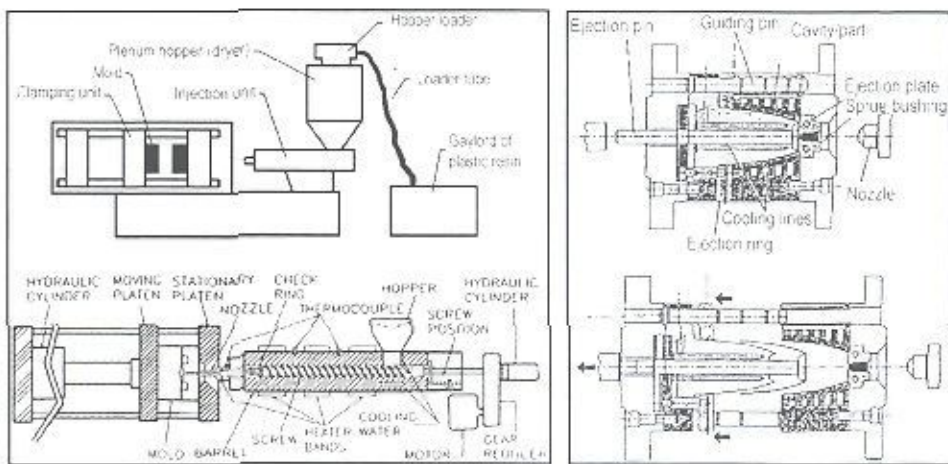


Figure 4: Schematics of an injection molding machine (left) and a mold (right).

Polymer melt is delivered into the mold by injection (Figure 4) This injection describes the start of a cycle that is basically divided in seven steps (Figure 5).

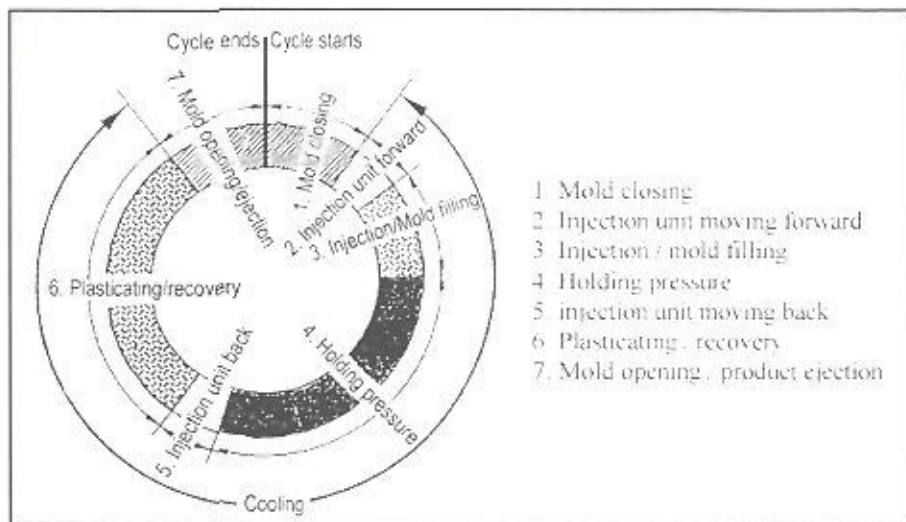


Figure 5: Injection molding cycle process.

As the injection molding procedure is a cycling process and the molds can be used immediately again after product ejection, the injection molding process offers a rapid method for polymer processing [7].

Other processing methods for polymeric materials are compression, transfer and blow molding, calendering and thermoforming [5,7].

1.5 Modification of Polypropylene

Specialized applications of polymers often require enhanced properties. In the case of polypropylene, changes in physical or chemical properties may be realized. These modifications can be performed before, during or after the processing step.

1.5.1 Modification Methods During Polymerization and Processing

Copolymerization is frequently used to change the physical and chemical characteristics of polymers by combining a second kind of monomer during the polymerization process. The addition of a second type of monomer usually changes the physico-chemical properties of the resultant product. Catalysts influence the copolymerization significantly.

In the case of polypropylene, a commercially produced copolymer is the so-called Impact Polypropylene. Impact polypropylene is produced by copolymerization of propylene with small amounts of ethylene as the copolymer. For this kind of copolymerization $MgCl_2$ -supported $TiCl_4$ catalyst with triethyl aluminum as cocatalyst are used [8]. Impact polypropylene features enhanced impact strength and dimensional stability compared with normal polypropylene.

Another possibility to modify polypropylene is to crosslink the macromolecular chains during production. Various procedures may be used to initiate crosslinking. Common ways of crosslinking consists of macroradical formation via thermal decomposition of organic peroxides, high energy irradiation (gamma or electron beam) and ultraviolet radiation in the presence of ultraviolet-sensitizers [9]. The formation of polypropylene macroradicals is easily initiated by more or less any radical initiator, except non-methyl alkyl radicals, as they are not reactive enough to initiate an efficient macroradical formation in polypropylene.

Oxyl radicals, formed by thermal decomposition of peroxides, are the most convenient radical species for polypropylene crosslink initiation. The macroradicals can decay by several ways (Figure 6) [10]. Polypropylene afforded by crosslinking show an

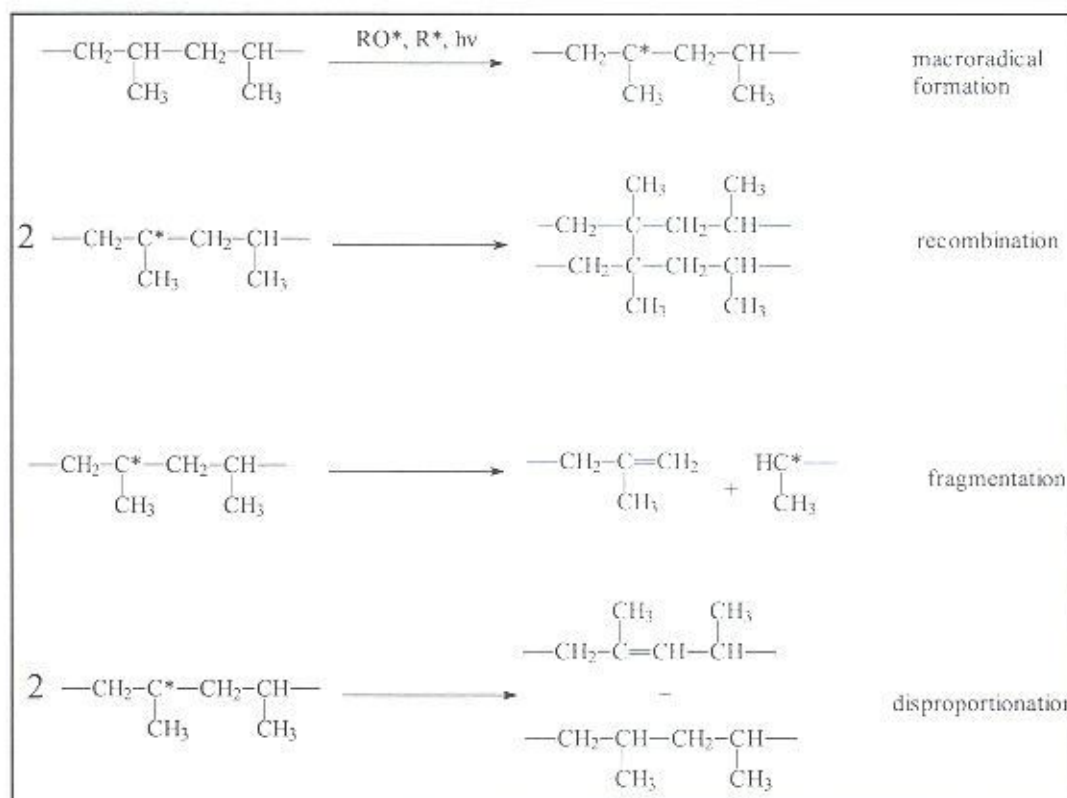


Figure 6: Radical mechanisms during crosslinking of polypropylene.

improvement in the impact resistance at low temperature and a decreased brittle-ductile transition temperature. Also the heat resistance of crosslinked polypropylene is increased significantly. Various applications are amenable to crosslinked polypropylene. For example, crosslinking to a gel content of 55% proved to be beneficial for cable insulation.

Further polypropylene can be modified during extruding or injection molding by including additives. Additives influence many physico-chemical properties. Those influencing the physical properties of polypropylene are generally called fillers. Fillers such as glass fibers, talc and calcium carbonate are added during processing to improve the stiffness, the heat deflection temperature (HDT) or the heat conductivity [5].

In contrast, additives like fatty acids, unsaturated dicarboxylic acids, surfactants, organic peroxides and ketones are added to influence the chemical properties of modified polypropylene. Using these additives, more polar polypropylene surfaces are created, affording higher wettability, adhesion and dyeability [11].

1.5.2 Modification Methods After Processing

Polymers such as polypropylene have low surface energies and therefore tend to be very inert. Thus it is helpful to modify the surfaces of polypropylene prior to processes like bonding, coating, printing or metallization. Frequently used surface treatments after forming-processing of polypropylene include plasma, corona and flame treatment.

Plasma treatment of polypropylene is an attractive process to produce the required surface modification by using different types of gas, introducing various chemical functionalities on the surface. A plasma can be broadly defined as a gas containing one or more charged and neutral species of electrons, positive ions, negative ions, radicals, atoms or molecules. Cold plasmas are formed, as a volume of gas is exposed to an electric field under low pressures. To produce plasma conventional frequencies, radio waves or microwaves may be used. The basic plasma reactor includes a vacuum chamber equipped with a gas source and electrodes (Figure 7). Reactions may occur between gas-phase

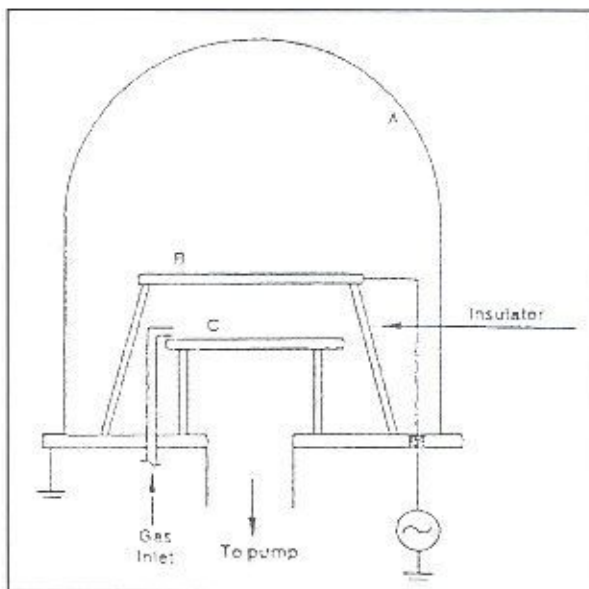


Figure 7: Schematic diagram of a laboratory scale plasma unit with a vacuum chamber (A), a RF-electrode (B) and a grounded electrode (C) [12].

and surface species to afford reactive functional groups or alternatively, may occur solely among surface species, affording crosslinks. Example reactions include plasma treatment by argon, ammonia, oxygen and water. Oxygen containing plasmas react with polypropylene, affording various functional groups including alcohols, ketones and carboxylic acids. Excellent results in plasma-treated polypropylene can be achieved using water/air (80:20) plasmas. However, plasma treatment has not been used as extensively as corona or flame treatment in industry, as plasmas are formed under vacuum conditions, which introduce higher expenses. Corona and flame treatments are used commonly because of their speed and ease of processing to improve bondability and printability of polyolefin films and large-sized objects.

A corona treatment system consists of an electrode connected to a high-voltage source and a electrically grounded roll usually covered with insulating material like

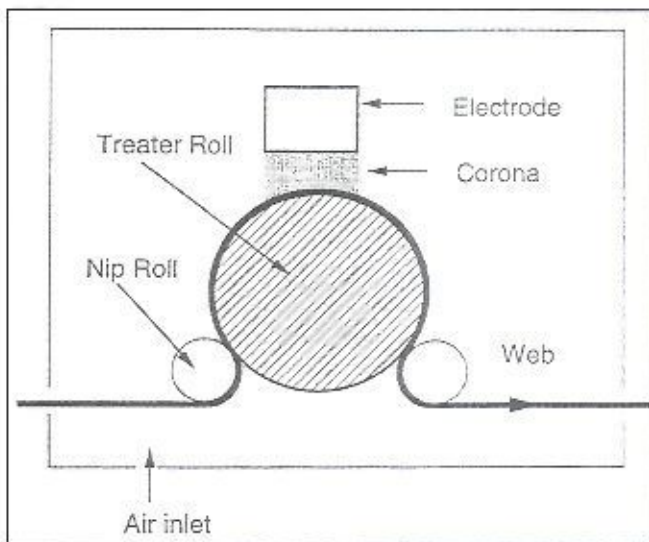


Figure 8: Schematic diagram of a corona discharge apparatus.

polyester (Figure 8). The corona is afforded when a high voltage is applied across the electrodes to cause ionization of air. This atmospheric pressure plasma is called a corona discharge. The insulating material, covering the grounded roll, prevents arcing between the two electrodes. As the corona is in contact with a polymer surface, it can cause the surface to oxidize. Electrons, ions, excited neutrals and photons which are present in a discharge can react with a polymer surface to form radicals. These radicals react rapidly with atmospheric oxygen (Figure 9). These reactions cause possible crosslinking and

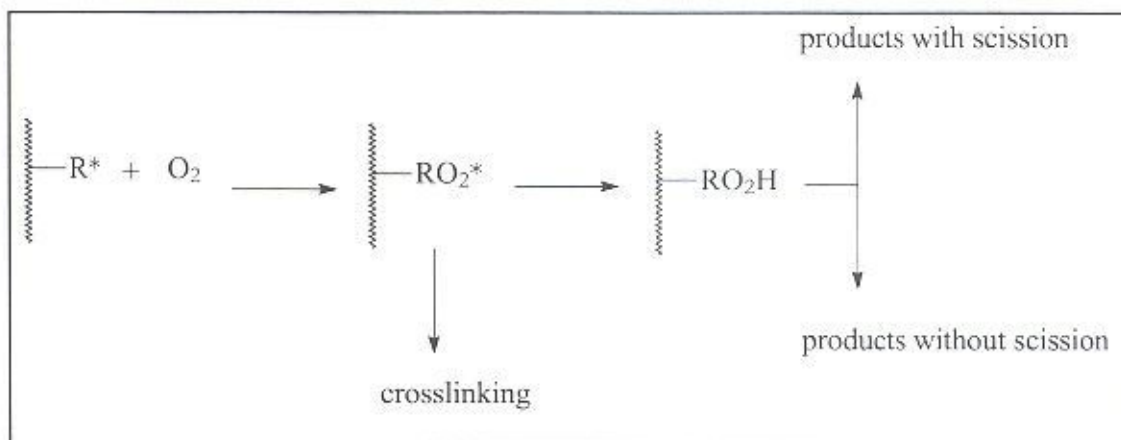


Figure 9: Reaction scheme of corona discharge introduced surface reactions.

functionalization of the polymer surface with and without concomitant chain scission. The decomposition of the hydroperoxide groups produces oxygen functional groups on the surface including alcohols, ketones and carboxylic acids.

Flames have been used in various industries for surface treatment of plastic. This technique has been proven convenient for specialized applications as the torches are portable. Flame treatment has also been employed to enhance ink performance of polymer surfaces. A flame treatment apparatus generally consists of a torch, a cooled backing roll and a nip roll to deliver the polymer film (Figure 10).

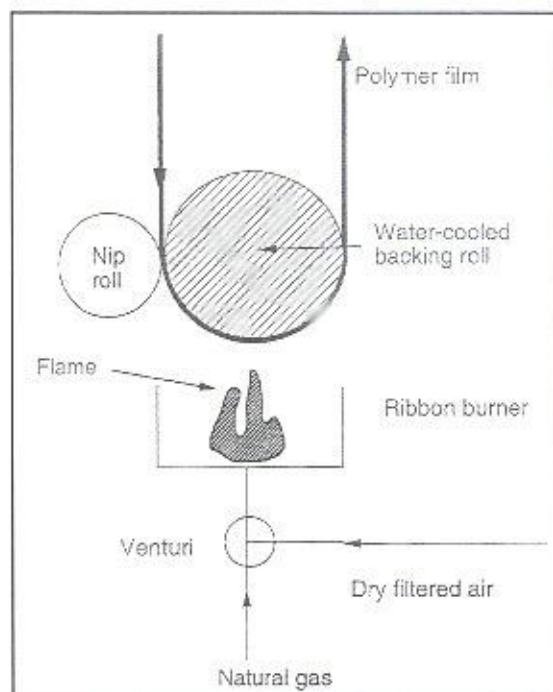


Figure 10: Schematic diagram of a flame treating apparatus.

Important variables for flame treatment are the air-to-gas ratio, air and gas flow rates, the distance between the tip of the flame and the surface, the nature of the gas and the treatment time. Oxidation at the polymer surface caused by flame treatment can be attributed to the high flame temperature (1000-2000°C) or reactions with many excited species in the flame. These reactions afford surfaces bearing alcohols, aldehydes, esters and

carboxylic acid groups pendant on methyl group of polypropylene (Figure 11) [13].

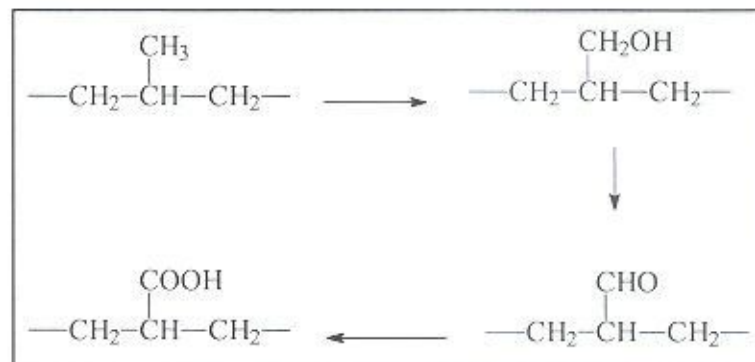


Figure 11: Reaction scheme of flame-treatment-mediated surface reactions.

Corona and flame treatments are very effective in oxidizing PP. Flame treated surfaces show the lowest advancing contact angle and the highest wettability.

1.6 Novel Modifications of Polypropylene

In light of this discussion, polypropylene appears to show great potential. However, the technology to implement its use in even larger scope has not been fully developed. It follows that a logical step in the development of polypropylene as a lucrative material is to find ways to introduce its use in the high-technology sector. The work covered in this thesis investigates potential and merit of surface engineering as a tool to adept the use of pre-manufactured polypropylene articles in life-science applications.

Chapter 2 discusses various oxidation routes to afford surface-active polypropylene. Chapter 3 discussed the use of pseudo-glass coatings on oxidized polypropylene as a means of purifying mRNA. Chapter 4 generalizes the concept of coating oxidized polypropylene by extending the study to trimethoxysilylpropyldiethylenetriamine. In addition, all chapters examine to binding of protein to the engineered surfaces.

1.7 References

- [1] J. R. Fried, *Polymer Science and Technology*, Pearson Education, 1995
- [2] www.nationalgeographic.com, Natural Geographic Society, 1997
- [3] A. C. Albertsson, *Chairmans Statement*, Department of Polymer Technology Royal Institute of Technology, Sweden
- [4] PETKIM, *Annual report 2001*, Petrokimya Holding AS, Turkey
- [5] J. Karger-Kocsis, *Polypropylene: An A-Z reference*, Kluwer academic Publishers, London, 1999
- [6] www.efunda.com/, eFunda Inc., Sunnyvale, USA, 2002
- [7] www.tut.fi/public/, Tampere University of Technology, Tampere, Finland, 2002
- [8] P. Kittilsen, T. F. McKenna, *Study of the Kinetics, Mass Transfer and Particle Morphology in the Production of High-Impact Polypropylene*, J. of Applied Polymer Science, 82(5), 2001
- [9] M. Lazár, R. Rado, J. Rychlý, *Crosslinking of polyolefins*, Adv. Polymer Science, 95, 1990
- [10] E. T. Denisov, *Reactivity of polyfunctional compounds in radical reactions*, Usp. Khimii, 54, 1985
- [11] H. Ishii, H. Takamatsu, Y. Hirayama, N. Kono, Jpn. Kokai Tokkyo Koho, JP 01 279 939, 1989
- [12] R. J. LaPorte, *Hydrophilic polymer coatings for medical devices*, TECHNOMIC Publishing Co., Inc., Lancaster, 1997
- [13] I. Sutherland, D. M. Brewis, R. J. Heath, E. Sheng, Surface Interface Anal., 17, 1991

Chapter 2: First Generation Surface: Oxidation of Polypropylene using Persulfate

2.1 Introduction

The importance of polymers in life science applications had grown over the last years to the point where polymers are used in every kind of application from simple storage purposes to highly engineered intelligent plastics. For general-use applications as reaction tubes, pipette tips, work surfaces and stands, standard polymers like polystyrene, polypropylene and polyester are used to produce unbreakable, light, convenient and practical laboratory equipment. These articles are generally intended for single-use.

More specialized polymers are normally used in specialized applications, often featuring attended and tailored physico-chemical surface properties. Examples include high-area surfaces, antimicrobial surfaces, biologically active surfaces for Enzyme-Linked Immunosorbent Assay (ELISA) applications and bio-passivated coatings for implants. In realizing these applications, the polymers have to be modified because the unmodified polymers are simply inadequate and do not give the desired effects. The production route of these surfaces was described previously and often requires specialized equipment.

The advantage of the method developed herein for polypropylene modification is exemplified by the ease which novel materials may be processed. As a source of polypropylene, Eppendorf reaction tubes were chosen, because these or similar polypropylene tubes are available in every standard laboratory. Based solely on aqueous reactions mediated by persulfate, there is no need for special laboratory equipment or knowledge of special reaction procedures. Simply put, the performed modification is adoptable to every kind of research laboratory and can be performed by any laboratory staff member. When considering the expense of commercially available analogs, the cost-efficiency is also an added benefit.

2.2 Materials and Methods

Tubes, Chemicals and Proteins

Polypropylene Safe-Lock Tubes (2ml capacity) were obtained from Eppendorf AG. Ammonium peroxodisulfate (98%) was purchased from Lachema, A. S., NERATOVIC. Standard grade isotactic polypropylene powder, bovine serum albumin and 5-dimethylamino-1-naphthalenesulfonyl chloride (dansyl chloride) were purchased from Sigma-Aldrich Laborchemikalien GmbH. Dialysis bags (3500 molecular weight cut-off) were obtained from Pharmacia. Deionized water ($18\text{M}\Omega/\text{cm}^3$) was produced in-house using a Millipore Academic system.

2.2.1 General Methods (GM):

(i) Preparation of Persulfate and Control Solutions

Ammonium peroxodisulfate solutions (APS) were prepared by dissolving the required amount of APS in water with the help of an ultrasonic bath and a VELP Vortex model Scientifica. In preparing control solutions, APS was replaced with the appropriate amount of ammonium sulfate, to remove the active agent, while still maintaining counterions and comparability. The solutions were freshly prepared before each experiment for the sake of maintaining consistency.

(ii) Reaction Method

The reactions were performed using a standard laboratory oven, a Savant Speedvac with the vacuum accessory disabled and an Eppendorf brand thermomixer. The chosen reaction temperature (70°C) was suitable for the activation of APS but not so high as to potentially alter the morphological properties of PP.

(iii) Washing and Drying Method for Modified Eppendorf Tubes

At pre-selected time points, samples were removed from the heating device and allowed to cool to room temperature. The remaining solutions were withdrawn and the emptied tubes were transferred into a glass bottle (Figure 12). This bottle was filled with deionized water and agitated to wash the tubes along the inner and outer sides. The wash procedure was applied three times to every lot of tubes, before they were dried *in vacuo* (70°C , 16h) in a NÜVE brand vacuum oven.

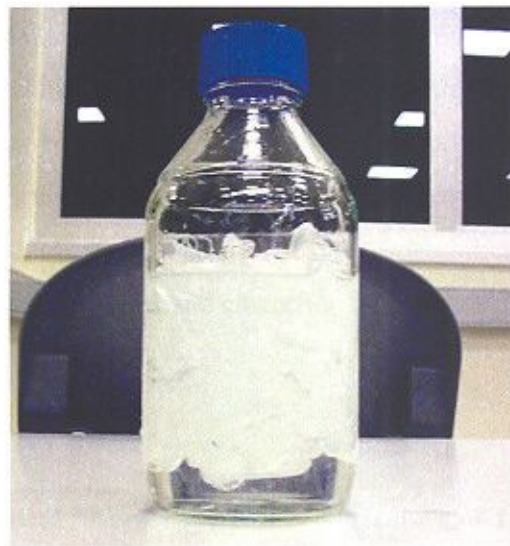


Figure 12: Typical set-up to perform washings during oxidation.

(iv) Preparation and ATR-FTIR Analysis of Eppendorf Tubes

Eppendorf Tubes were prepared in a way that would permit effective analysis using the attenuated total reflectance (ATR) accessory of the FTIR instrument. As excessive bending of samples during the sample preparation yielded poor ATR-FTIR spectra, this modification to the method was introduced to protect the crystal structure of the polymer. A cylindrical piece with an approximate height of 3mm was cut from a region just above the hemispherical base of the tube using a razor blade heated in a Bunsen burner. The cylindrical ring was frozen in liquid nitrogen and shattered into small pieces with approximate dimensions of 2x3mm (Figure 13),



Figure 13: Sample preparation for ATR-FTIR measurements (cutting steps).

These pieces were then *in vacuo* (40°C, 2h). Samples prepared in this way had little or no damage to the crystal structure but nevertheless some bore thick edges, which arose from the cutting action of the hot blade. These regions were carefully exercised with a flat-edged razor blade. The samples were tightly fixed over the measurement window of the ATR accessory of a Bruker model Equinox 55 infrared spectrophotometer. Twenty scans were averaged and displayed using rubber-band correction at 70 points in the Bruker OPUS V3.1 software of the system.

(v) Preparation and Optical Microscope Characterization of Tubes

For the optical microscope analyses no special sample preparation like cutting or breaking of the tubes was required, so the inner wall of the tubes could be observed by appropriately focusing the microscope. In fact, by varying the focal length accordingly, different depths of penetration can be easily examined. Samples were analyzed using an

Olympus brand CH40 light microscope fitted with an Ikegami model CCD camera using a magnification of 100X. Photos were taken directly from the monitor of the CCD camera using a Sony Cybershot DSC-F505 digital camera (2.1 mega pixels). The quality of the pictures is limited by the resolution of the screen. As well, the interface of the monitor was necessarily captured using digital photography and proved slightly inconvenient.

(vi) Preparation and Scanning Electron Spectroscopy (SEM)

Sample tubes were prepared analogous to the method used for the ATR-FTIR analysis. These samples were cleaned and coated by gold inside an Agar brand sputter coater (25s), affording a coating with an approximate thickness of 20nm. Scanning electron micrographs were obtained using a JEOL model JSM-6500F microscope with beam energy of 10 to 20kV. At least four areas were examined per sample at magnifications up to 50000X. Images were displayed and processed using windows-based imaging software. Subsequent analyses were achieved using iridium as coating material (5nm) and a beam strength of 2kV.

(vii) Trace Dansylation of Bovine Serum Albumin (BSA)

Heat-shock fractionated BSA (100mg) was dissolved in water (10ml) and the pH value was adjusted to 9 using sodium hydroxide solution (1M). 5-Dimethylamino-1-naphthalenesulfonyl chloride (Dansyl chloride, 5mg) was dissolved in acetonitrile (100 μ l) and slowly added to the gently stirring BSA solution maintaining the pH value between 8 and 9 using sodium hydroxide solution. After 1h, the solution was delivered into a dialysis bag and dialyzed (25°C) against 3x4L water. Ninhydrin color analysis of native albumin and dansylated albumin indicated that at most 10% of the amino groups had been transformed into the sulfonamide fluorophore. The dansylated protein was stored at 4°C.

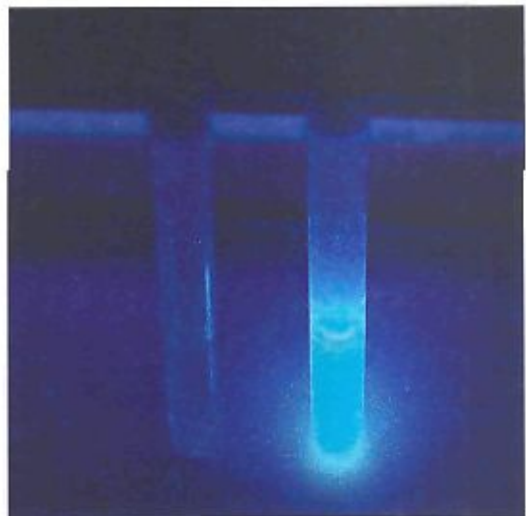


Figure 14: UV-photograph of native (left) and dansylated BSA (right).

(viii) Immobilization Method for Trace Dansylated Protein UV Analyses

A portion of the dansylated BSA stock was added to excess salt solution (1M NaCl) in order to afford a dilute stock (0.3mg protein/ml, pH 7) that would be appropriate for immobilization studies. This solution was transferred in the modified tubes and incubated (37°C, 1.5h). The solution was withdrawn, and the residing liquid was pooled by centrifugation and collected using a pipette. Photographs were obtained using an Uvitec UV-box quipped with an Ihi CCD camera. The tubes were filled with aqueous sodium chloride solution (1M, 1ml) and agitated (2min). The washing solution was withdrawn and the tubes were again photographed. Next, the tubes were washed with water and similarly documented. After that, the same washings were performed with 10% Triton X100 and 10% NP-40 solutions. Photographs were taken after every washing.

2.2.2 Analyses of Starting Polymer: Eppendorf Safe-Lock Tubes

(i) Scanning Electron Microscopic (SEM) Analyses of Native Surfaces

Native samples were treated the as described before (GM) except, the native samples were coated using silver. The results show good image contrast between the surface and the air. No differences between gold and silver coating were observed.

(ii) X-ray Powder Diffraction Analysis of Native Eppendorf Tubes

Tubes (~20mg) were dried under vacuum (70°C) and fragmented using a standard coffee grinder. Again, to minimize anomalies introduced by deformation during the sample preparation, the tubes were first frozen in liquid nitrogen. The collected fragments were sieved, using mechanical sieves, to obtain samples of 1-2mm and less than 1mm particle size. Samples with a particle size of 1-2mm (1-2g) were analyzed using a Bruker AXS Advance powder diffractometer, equipped with a Siemens X-ray gun. The measurement was performed with a rotation speed of 15rpm through an angle of $2\theta = 10 - 90^\circ$ using the default parameters set by the Bruker AXS Diffrac PLUS software. An X-ray generator setting of 40kV and 40mA was employed.

(iii) Differential Scanning Calorimetry (DSC) of Native Eppendorf Tubes

Samples intended for DSC analyses were prepared in the same way as samples examined by X-ray. Both obtained samples sizes were analyzed under nitrogen atmosphere in a Netzsch brand model 204 DSC system equipped with a DSC 204 cell and a Netzsch TASC 414/4 controller unit. The temperature was ramped from - 80°C to 210°C at a rate of 10°C/min. Data was collected using Netzsch TA4 software.

(iv) ATR-FTIR Analysis of Native Eppendorf Tubes

Native Eppendorf Tubes were prepared for ATR-FTIR analyses as described previously (GM). Spectra of these samples and of commercially obtained isotactic polypropylene powder were compared against the Aldrich FTIR Library.

2.2.3 Oxidation Experiments

To achieve the optimum concentration and reaction time for the oxidation of the polypropylene surfaces a concentration course and a time course of the reaction was performed in the beginning.

(i) Concentration Course

Different concentrations of aqueous ammonium peroxodisulfate (APS) were prepared (0.5, 1, 1.5, 2, 2.5 and 3 M). An equal volume of each solution (1.5ml) was transferred into a native Eppendorf Tube using an Eppendorf Multipette Plus. These tubes were then placed in a tube rack and incubated in a standard oven. The tubes were appropriately restrained (Figure 15) to prevent caps from opening by the accumulation of pressure during reaction (70°C, 24h).



Figure 15: Set-up used to restrain caps during the course of oxidation.

After the reaction the tubes were washed, dried (GM) and tested visually using the loading of trace-dansylated BSA (GM) as an arbitrary indicator of the extent of reaction. On the basis of fluorescence intensity, the best “oxidation” was assigned to 1M persulfate and all subsequent reactions were carried out at this concentration. Native and oxidized tubes were also examined visually as control tubes. ATR-FTIR analyses were not performed, as these experiments were the most preliminary of all studies and the protocol to prepare samples for ATR-FTIR analysis had not been developed by that time.

(ii) Time Course

In light of the results of the concentration course, 1M solutions of APS were used. APS (11.82g) was dissolved in deionized water (50ml) giving a clear solution. This solution (28.5ml) was equally divided into Eppendorf Tubes (19). The tubes were fixed in an oven (Figure 15) and incubated (70°C, 24h). During the first 18h of reaction, a tube was removed every hour. The last tube was removed after 24h. The tubes were immediately washed, dried, prepared and analyzed by ATR-FTIR using the previously described methods (GM).

After interpreting the results of the concentration and time course experiments, the optimum reactions conditions were ascertained (1M, 70°C, 16h) and applied to all subsequent experiments.

(iii) Oxidation of Tubes under Static Conditions

Persulfate and sulfate standard solutions were administered (1.5ml) to tubes as discussed previously (GM). The tubes were fixed in a rack in the oven. The reaction was performed using optimum parameters (1M APS, 70°C, 16h). The reaction tubes were rinsed and prepared for the Optical microscopy, ATR-FTIR and SEM analyses using standard procedures (GM). Protein immobilization tests using dansylated BSA were carried out as an arbitrary measure of the performance of the new surfaces.

To estimate the penetration depth of oxidation, a sample was prepared using standard methods for ATR-FTIR sample preparation (GM). Series of adjacent layers comprising the plastic wall was incrementally removed from this sample using Egeli brand fine gauge (1200c) sandpaper. Commencing at the reacted surface and working inwards, the composition of underlying functional groups after every successive removal of 8-12 microns of material was assessed directly using ATR-IR spectroscopy. The corresponding reduction in sample wall thickness, and by inference, the depth of each measurement, was quantified using a Mitutoyo brand digital caliper.

(iv) Oxidation of Tubes in a Rotating Speedvac Concentrator

As the modification using a standard oven proved inconvenient because of the need to fix the tubes as well as several incidents in which tubes popped under pressure, another method was developed to oxidize the native tubes. For this purpose, a Savant brand speedvac, with its vacuum accessory disabled was used. APS and sulfate-control solutions were prepared as noted previously (GM). Tubes were loaded into the speedvac rotor and filled to capacity with the reaction solutions. The speedvac was preheated (70°C) and water

(~150ml) was added into the rotor chamber (Figure 16). In this humid atmosphere the tube-loaded rotor was fastened and spun, while the lids of the tubes remained open. The delivery of the samples into the speedvac, during which time the lid was opened, was rapid to minimize the loss of humidity in the atmosphere.



Figure 16: Preheated speedvac showing humid atmosphere used to minimize evaporation from tubes.

Reaction (70°C, 16h), washing and drying procedures, optical microscopy, ATR-FTIR and SEM analyses, and protein immobilization studies were all performed as noted previously (GM).

(v) Oxidation of Tubes in a Rotating Thermomixer

While the previously performed reactions were performed under static conditions or under the influence of minor vibrations, a novel method was introduced to perform oxidations with efficient mixing.

For this purpose Eppendorf Tubes were mounted in the rack of an Eppendorf Thermomixer. The tubes were filled with freshly prepared APS (1M) or sulfate-control solutions (1.5ml). The oxidation reaction was performed using mixing (500rpm) and standard parameters (70°C, 16h). After reaction, tubes were rinsed and dried as previously described (GM). Following standard sample preparations (GM), optical microscopy, ATR-FTIR and SEM analyses were performed.

To compare the performance of these surfaces with the previous ones, fluorescent BSA was incubated on these surfaces and optical UV-analyses were performed.

2.3 Results and Discussion

(i) Analyses of Native Eppendorf Tubes

All Save-Lock brand Eppendorf Tubes are injection-molded plastics purported to be composed of crystalline, non-crosslinked and non-reacted isotactic polypropylene. To validate this information, initial efforts of this study were invested in assessing the starting material.

Scanning electron microscopic analysis of the native samples showed typical characteristics of injection molded polymers. In particular, inner and outer regions of the wall cross-sections showed skin layers of an approximate 15-20 μm thickness. Skin layers caused by the rapid cooling of the melt during injection-molding procedures and display high smectic content. Underlying the skin layers, a shear layer and core region could be detected. These morphologies are typical for injection-molding processed PP. [1, 2]

Powder X-ray diffraction spectra of the tubes (Figure 17) were compared to standard polymorphs of isotactic PP. These indicated that the dominant crystal structure by volume was the alpha-form of which the majority presumably lay in the core region of the tube walls. Also a small but characteristic signal of the beta-morph form of isotactic polypropylene could be observed. In light of the established properties of PP, the β -polymorph is likely located in the thin shear layer between the skin layer and the core region [1 – 4].

Gamma and smectic polymorphs could not be detected by diffraction studies, but this outcome was not surprising, as both polymorphs have usually a low content in material produced by injection-molding. [1]

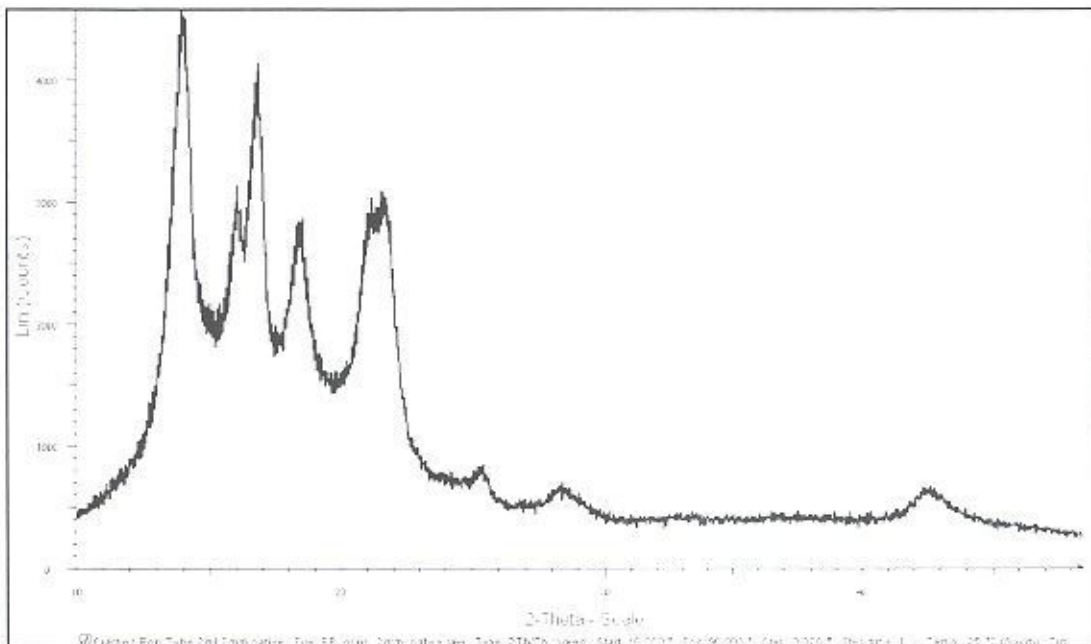


Figure 17: X-ray spectrum of native Eppendorf polypropylene tube fragments ($\phi = 1\text{-}2\text{mm}$).

DSC analyses validated the diffraction results in that the spectrum showed for the alpha polymorph an endotherm fusion peak at 168°C , while the beta endotherm, which describes usually a variable shoulder centered at 146°C , was in this example likely submerged under the alpha endotherm. DSC analyses also indicated a glass transition temperature inflecting at -5°C , which is typical for non crosslinked or isotactic polypropylene (Figure 18). [5, 6]

Comparisons of the reported enthalpy of 138J/g for isotactic polypropylene with the measured value of 88J/g results indicated that the crystalline content in the measured isotactic polypropylene was approximately 64%, which is a normal value for non-crosslinked, injection-molded polypropylenes [1].

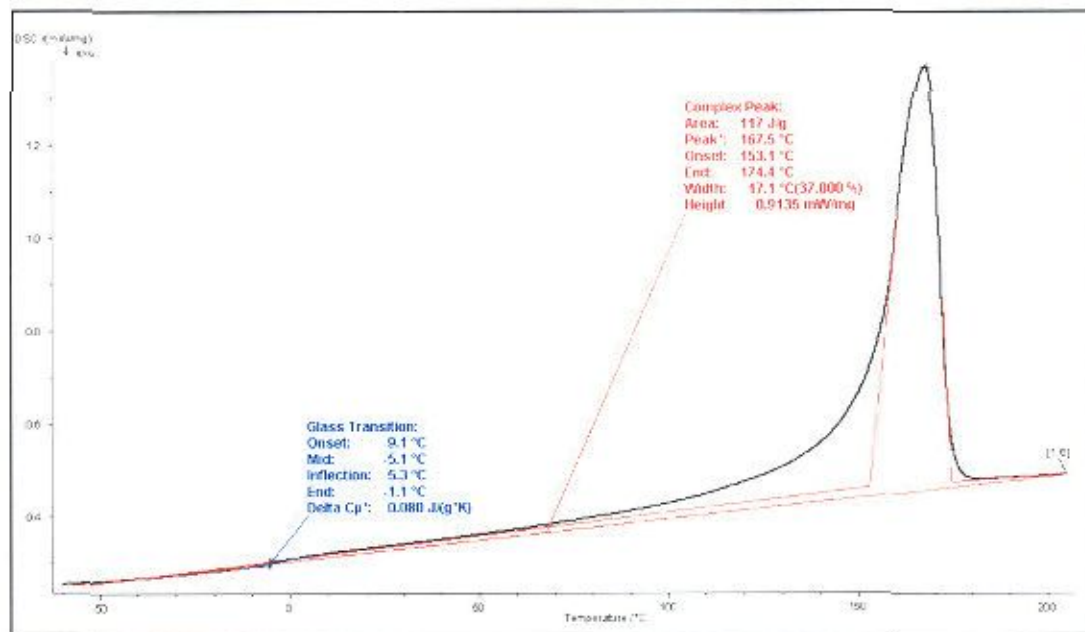


Figure 18: DSC spectrum of native Eppendorf polypropylene tube fragments ($\phi = 1\text{-}2\text{mm}$).

ATR-FTIR spectra of Eppendorf Tubes were cross-referenced against commercially available isotactic polypropylene powder (Figure 19). Both samples afforded comparable spectra and could be validated against spectral libraries (not shown) of isotactic polypropylene. The presence of significant amounts incipients or degradation products could not be observed during the analyses.

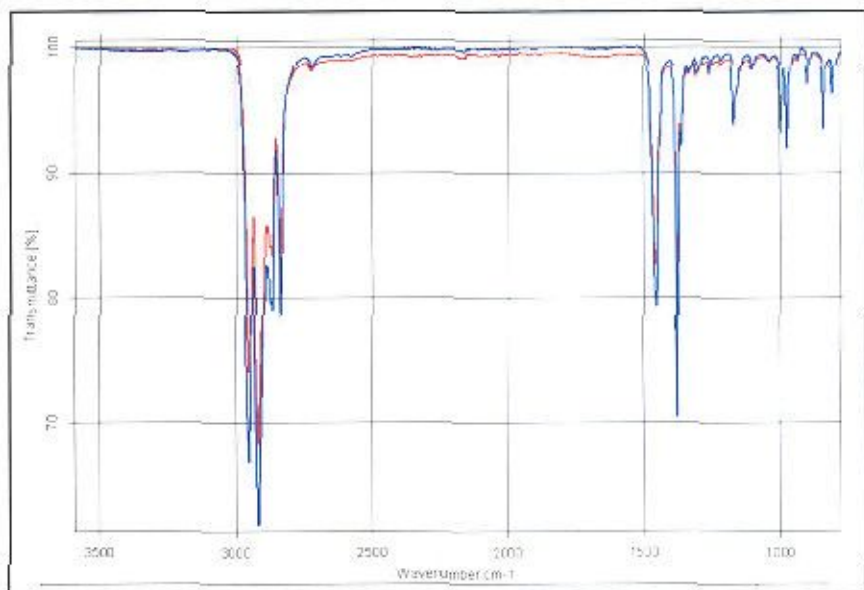


Figure 19: ATR-FTIR spectra of native Eppendorf Tubes (blue) and isotactic polypropylene powder (red)

The outcome of all analyses used to examine the Eppendorf Safe-Lock Tubes indicated that the starting material consisted out of high-quality, injection-molded isotactic polypropylene. [7]

(ii) Concentration Course

Visual analysis (Figure 20) and UV-analysis of fluorescent protein immobilized on the oxidized surfaces during the time-course experiment indicated, that APS solutions prepared in one molar concentrations offered the optimum reaction performance. No significant difference in the apparent immobilization of fluorescent protein could be observed using APS solutions of one or higher molarities. Concentrations of 0.5 molar APS solutions seemed not to be suitable for the reactions, because oxidized surfaces showed decreased protein binding compared to the higher concentration oxidized surfaces.

Considering these results, 1M APS was arbitrarily chosen to be the best concentration to perform an effective oxidation in a convenient time-frame.



Figure 20: Photograph showing the optical effect of the oxidation caused by different concentrations of persulfates during the concentration course
(Sets of tubes from left to right and top to bottom: 0.5M APS; 1M APS; 1.5M APS; 2M APS; 2.5M APS; and 3M APS).

(iii) Time Course

The ATR-FTIR spectra of the oxidation as a function of time illustrate the development of carbonyl absorptions with increased oxidation times. In particular, three absorbances of three major populations of carbonyl compounds ($\nu_{C=O} = 1705, 1735$ and 1770cm^{-1}) were noted, indicating the accumulation of oxidation products during the reaction (Figure 21) [8, 9]. Absorbances in the carbonyl region were chosen to quantify the reaction, as they showed the most significant changes during the course of reaction.

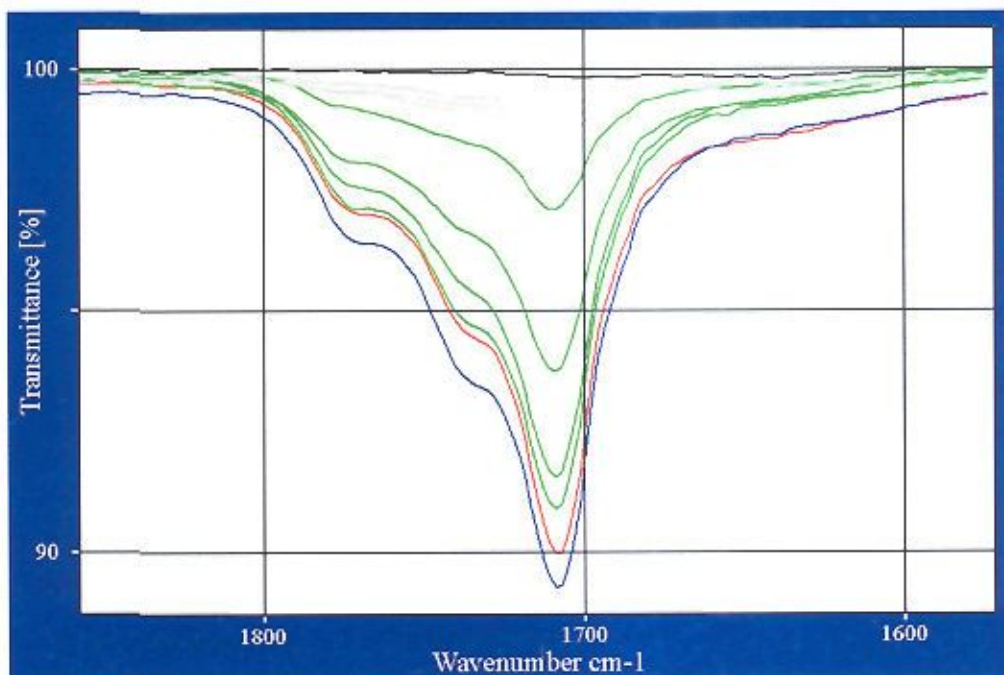


Figure 21: ATR-FTIR spectra of the time-course experiment. Grey lines indicate early stages of reaction (2-4h) and green lines indicate intermediate stages (6-12h). Blue depicts the optimum time (16h) and red suggests that product loss has begun (24h). Black is the control (native PP).

The accumulation of signal was gradual during the early and intermediate stages of the time course, suggesting a steady rate of overall reaction. More importantly, the consistent line shape at different time points appeared to suggest a steady accumulation of different products. The 16h profile denotes the time of maximum yield. At 24h, a decrease of signal

was in fact noted. This finding suggested that within the penetration range of the instrument, a highly oxidized fraction of material detached from the polymer, resulting in a net loss of signal. These results suggested that the optimum reaction time of the performed oxidation reaction was 16h.

(iv) The Nature of the Oxidation Reactions

All oxidation experiments herein (oven, speedvac, thermomixer) were analyzed and discussed on the basis of FTIR data and various additional chemical tests (results not shown).

ATR-FTIR spectra taken of samples afforded by the three modification protocols were very comparable in functionalization. This finding indicates that the modification method apparently has no influence on the chemical processes during incubation. In particular, no influence of stationary reaction, slight vibration or mixing conditions, could be noted on product distribution.

ATR-FTIR spectral profiles following treatment with APS solution differed in the functional group region ($4000\text{-}1300\text{cm}^{-1}$), the fingerprint region ($1300\text{-}900\text{cm}^{-1}$) and the remaining low-frequency region ($900\text{-}600\text{cm}^{-1}$) (Figure 22).

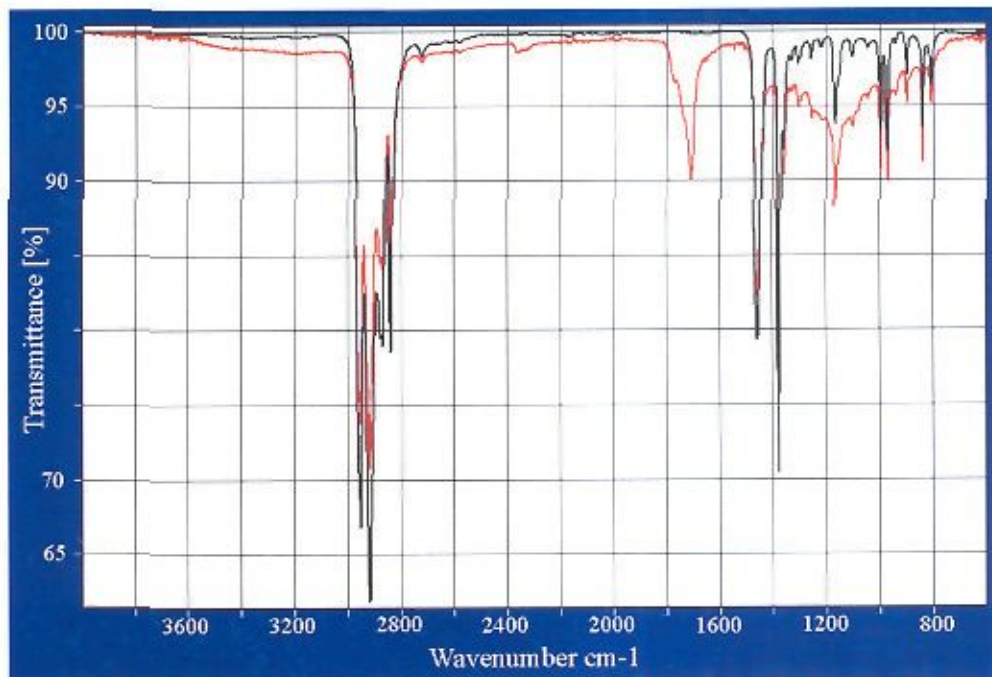


Figure 22: ATR-FTIR spectra of native (black) and oxidized (red) tubes.

The chemistry employed and spectral profile obtained was consistent with a number of functional groups. Ruling out candidates such as vinyl, peracid, peroxide, hydroperoxide and aldehyde, the products most likely formed alcohol ($\nu_{\text{freeH-O}} = 3640\text{-}3610\text{cm}^{-1}$; $\nu_{\text{H-bondedH-O}} = 3420\text{-}3250\text{cm}^{-1}$; $\nu_{\text{bendC-OH}} = 1440\text{-}1260\text{cm}^{-1}$; $\nu_{\text{C-O}} = 1160\text{-}1030\text{cm}^{-1}$), ketone ($\nu_{\text{C=O}} = 1725\text{-}1705\text{cm}^{-1}$), carboxylic acid ($\nu_{\text{freeH-O}} = 3550\text{-}3500\text{cm}^{-1}$; $\nu_{\text{H-bonded H-O}} = 3300\text{-}2500\text{cm}^{-1}$; $\nu_{\text{C=Omonomer}} = 1780\text{-}1740\text{cm}^{-1}$; $\nu_{\text{C-Odimer}} = 1710\text{-}1690\text{cm}^{-1}$; $\nu_{\text{stretchC-O}} = 1320\text{-}1210\text{cm}^{-1}$; $\nu_{\text{bendC-OH}} = 1440\text{-}1400\text{cm}^{-1}$), ether ($\nu_{\text{C-O}} = 1140\text{-}1110\text{cm}^{-1}$) and ester ($\nu_{\text{C-O}} = 1765\text{-}1720\text{cm}^{-1}$; $\nu_{\text{C-Oacid}} = 1280\text{-}1150\text{cm}^{-1}$; $\nu_{\text{C-Oalcohol}} = 1150\text{-}1000\text{cm}^{-1}$) [8 - 13].

The immediate goal was to summarize by means of an overly simplified mechanism that the products stated above could in fact be afforded. The oxidation

$\frac{1}{2} \text{O}_3\text{SO}-\text{OSO}_3^- \rightarrow \cdot\text{SO}_4^- + \text{H}_2\text{O} \rightarrow \cdot\text{OH} + \text{HSO}_4^-$	(1) homolytic decomposition
$\text{RH} + \cdot\text{OH} \rightarrow \text{R}\cdot + \text{H}_2\text{O}$	(2) initiation
$\text{R}\cdot + \text{O}_2 + \text{HR}^{\cdot} \rightarrow \text{R}-\text{OO}\cdot \rightarrow \text{R}-\text{OOH} + \cdot\text{R}^{\cdot}$	(3) propagation
$\text{R}-\text{OOH} \rightarrow \text{R}-\text{O}\cdot + \cdot\text{OH}$	(4) thermal decomposition
$\text{R}-\text{OOH} + \text{HOO-R}^{\cdot} \rightarrow \text{R}-\text{O}\cdot + \cdot\text{OO-R}^{\cdot} + \text{H}_2\text{O}$	(5) thermal decomposition
$\text{R}-\text{O}\cdot \rightarrow \text{R}=\text{O} + \cdot\text{R}^{\cdot}$	(6) scission
$\text{R}-\text{OOH} + \text{H}^{\cdot} \rightarrow \text{R}=\text{O} + \text{HO-R}^{\cdot}$	(7) acid catalyzed decomposition
$\text{HR}-\text{OOH} + \text{H}^{\cdot} \rightarrow \text{R}=\text{O} + \text{H}_2\text{O}$	(8) acid catalyzed decomposition
$\text{HR}-\text{OOH} + \cdot\text{OOR}^{\cdot} \rightarrow \text{R}=\text{O} + \cdot\text{OH} + \text{HOO-R}^{\cdot}$	(9) radical decomposition
$\text{HR}-\text{OOH} + \cdot\text{OH} \rightarrow \text{R}=\text{O} + \cdot\text{OH} + \text{H}_2\text{O}$	(10) radical decomposition
$\text{R}=\text{O} + \cdot\text{OH} \rightarrow \text{R}(\text{=O})\text{OH} + \cdot\text{R}^{\cdot}$	(11) transfer
$\text{R}=\text{O} + \cdot\text{OR}^{\cdot} \rightarrow \text{R}(\text{=O})\text{OR}^{\cdot} + \cdot\text{R}^{\cdot}$	(12) transfer
$\text{RH} + \cdot\text{O-R}^{\cdot} \rightarrow \text{R}\cdot + \text{HO-R}^{\cdot}$	(13) transfer
$\text{R}\cdot + \cdot\text{O-R}^{\cdot} \rightarrow \text{R-O-R}^{\cdot}$	(14) termination
$\text{R}\cdot + \cdot\text{OH} \rightarrow \text{R-OH}$	(15) termination
$\text{R}-\text{OO}\cdot + \cdot\text{OO-R}^{\cdot} + \text{H} \rightarrow \text{R-OH} + \text{O=R}^{\cdot} + \text{O}_2$	(16) termination
$\text{RO}\cdot + \beta-\text{H}_2\text{O} \rightarrow \text{R-OH} + \text{O=R}^{\cdot} + \text{O=R}^{\cdot}$	(17) termination
$\text{HR-O}\cdot + \cdot\text{OH} \rightarrow \text{R}=\text{O} + \text{H}_2\text{O}$	(18) termination

is initiated by homolytic decomposition of persulfate (1). Hydrogen abstraction from water by the sulfate radical anion follows, affording a hydroxyl radical as major initiator (1) [12]. The hydroxyl radical may then abstract a surface-pendent hydrogen atom, typically from a tertiary carbon, to afford an alkyl radical (2) [12, 13]. Rapid addition of oxygen, followed by peroxy radical-mediated hydroperoxidation, is realized in the propagation phase (3) [18, 23]. Propagation can lead to either isolated or clustered hydroperoxides. The extent of clustering is influenced by the efficiency of an intramolecular backbiting reaction that leads to the generation of new tertiary, secondary and primary carbon radicals, of which secondary radicals describe the majority. Hydroperoxide decomposition may be achieved by homolytic thermal breakdown (4, 5), acid catalyzed transformation (7, 8), and radical abstraction of the α -carbon hydrogen (9, 10). Monomolecular thermolysis (4) and

bimolecular thermolysis (5) are both plausible in this system and lead to chain branching [18, 22; 13, 20, 22]. Hydroperoxide thermolysis (4, 5) can induce main-chain scission, affording an end-chain ketone fragment and carbon radical (6), side-chain scission, affording an in-chain ketone and methyl radical (6) [1, 15, 16, 13, 19], and dehydration in the case of secondary hydroperoxides, affording an in-chain ketone (18). Heterolytic bond cleavage via acid catalysis affords chain scission, an end-chain ketone fragment and end-chain alcohol fragment (7), or dehydration, with in-chain ketone formation (8) [15, 21; 15]. Carboxylic acids may also catalyze homolytic bond cleavage via a 6-membered cyclic transition state. α -Hydrogen abstraction by peroxy radical leads to spontaneous hydroperoxide breakdown and ketone formation (9) [15]. It follows that a similar reaction mediated by hydroxyl radical (or even alkoxy radical) may occur in selected regions of polypropylene under the experimental conditions employed (10) [19, 24]. As hydroxyl radical and ketone are co-produced (8, 9), their juxtapositioning could promote the formation of carboxylic acid (11) [13, 17]. The effectiveness of this transformation is anticipated, as the two components may be unable to separate quickly and therefore mimic the cage effect that is known for viscous polymer melts. The production of esters by a similar radical transfer process (12) has been discussed [13, 17]. In addition to ketone and ester formation, the alkoxy radical contributes to alcohol formation via hydrogen abstraction and radical transfer (13) [18, 19, 20, 22]. Related hydroxyl-mediated transfer reactions, identical to initiation (2), also occur. Termination is governed by the homolytic recombination of hydroxyl, alkyl, alkoxy and peroxy radicals (14-18). Alkyl radicals are typically short lived, recombining with alkoxy radicals to afford ethers (14) or hydroxyl radicals to form alcohols (15) [11; 13, 14]. Secondary and tertiary peroxy radicals may co-terminate, affording alcohol and ketone (16) [24, 25]. Intermolecular hydrogen abstraction by alkoxy radical at the β -carbon of a secondary hydroperoxide affords alcohol, ketone and aldehyde, with concomitant chain scission (17) [13, 26]. Secondary alkoxy radicals in particular can also terminate via hydroxyl radical-assisted dehydration (18) [11, 26].

The oxidation may be generally viewed as a partially ordered, weight-averaged summation of radical-mediated propagation, transfer, scission, and termination pathways, as well as radical, thermal and acid-catalyzed peroxide decomposition pathways. The observed yields are of course subject to variation by any number of alternate pathways. Alcohol, for example, may be transformed by oxidation to carbonyl and even to carboxylic acid. Short-lived aldehydes are known to easily proceed to the carboxylic acid. Esters can also be produced by reaction of aldehyde and hydroperoxide precursors. Persulfate concentration, local oxygen availability, pH, temperature and polymer structure are some parameters that can influence the absolute and regional distribution of the four radical types and the final product distribution.

In interpreting the results of reaction with persulfate, another matter to point out is that attenuated total reflectance describes the state of sub-surface groups. With respect to achieving good surface bonding, however, only the nature of surface-exposed groups bears primary importance, as only those functional groups will define the choice of reagent used in the subsequent synthetic step. On the basis of the above discussion and the fact that reactions were initiated at the surface, the groups positioned thereon likely bear similarities to those noted in the immediate underlying layers. Surface-positioned carboxylic acid, ketone and hydroxyl groups in particular are very strong candidates. The longevity of ester groups in particular was questionable in light of acidic and hydrolytic conditions at the surface, which could afford additional acid and alcohol groups. Similarly, ethers were not considered, as they offered little advantage for synthetic purposes.

(v) Extent of Penetration of Oxidation

The penetration depth of the oven-mediated oxidation reaction was investigated using ATR-FTIR methods. The carbonyl region in particular was pre-selected as it bore the most notable changes. The ATR-FTIR spectra show a decrease of the complex carbonyl signal intensity with every successive removal of the topmost surface layer (Figure 23).

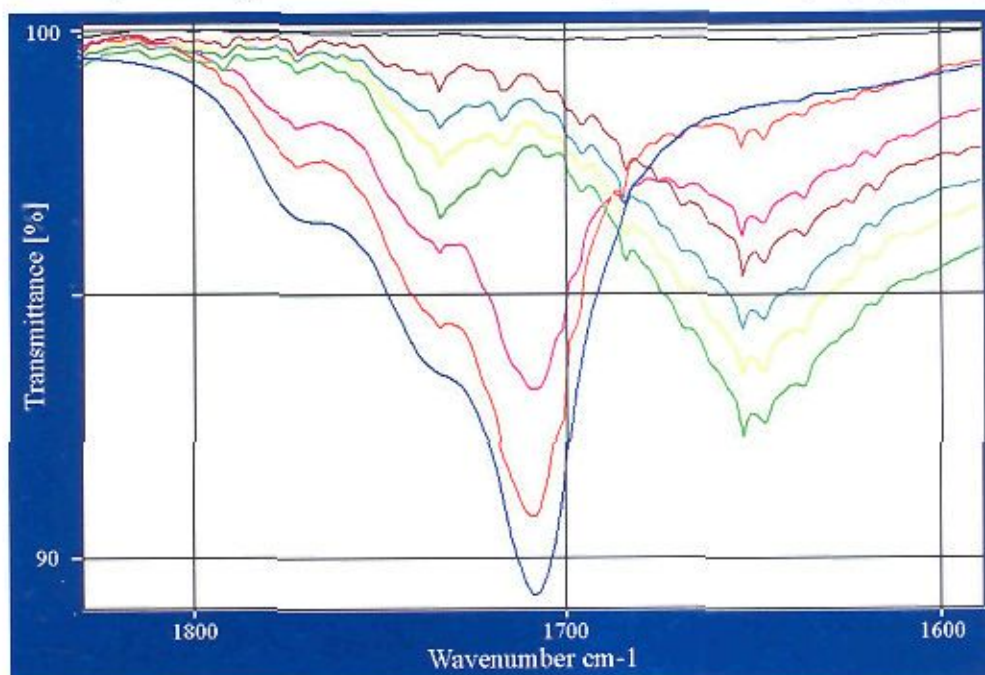


Figure 23: ATR-FTIR spectra of carbonyl region ($\nu_{C=O} - 1725-1705\text{cm}^{-1}$) illustrating the loss of carbonyl signal with increasing penetration depth

Each layer removed was approximately 10 microns in thickness, implying that the extent of oxidation had penetrated far deeper into the plastic than could be measured using the ATR accessory. The sequential debridement/ATR strategy therefore described a convenient method to assess the regional state of functional groups. By extrapolating to zero signal, the depth of oxidation was estimated at 100 microns penetration. Signals to the right of the carbonyl region were attributed to increasing amounts of sand paper residue impregnated in the plastic.

(vi) Microscopic Analyses

The oxidation reactions afforded tubes which showed not only a change in their chemical properties, but also a change of their physical surface properties. This change was readily apparent, because the tubes showed an optical effect after oxidation best described as slight whitening (figure 24). Ammonium sulfate reacted controls did not afford this physico-chemical change.



Figure 24: Opacity noted following oxidation
(left: control, right: modified).

Optical microscopic results pointed out, that this effect was caused by macroscopic parallel cracks in the skin layer, densely arranged and running horizontally along the walls of an upright tube (figure 25). Such cracks were only viewed in persulfate treated tubes and

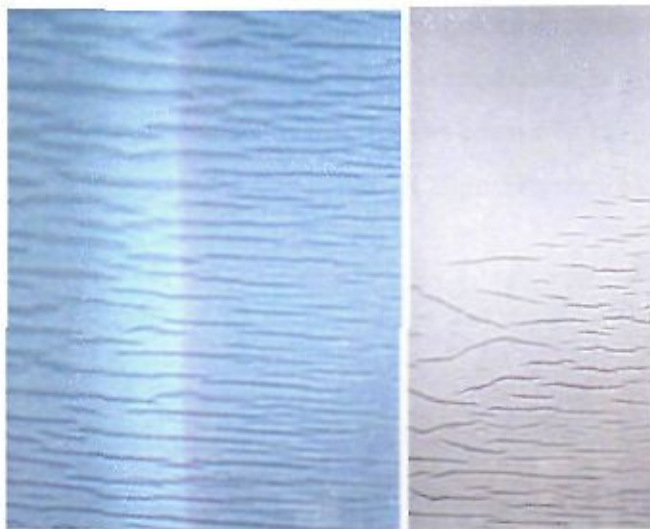


Figure 25: Macroscopic cracks seen in treated surfaces (left) and the cracking border between oxidized and unreacted surfaces (right) observed by optical microscopy.

more specifically were restricted to the areas having had direct contact with solution, precluding the effects of heat as a sole cause. Identical material above the solution line appeared normal. These densely clustered cracks measured on the tens of microns scale. Apart from the appearance of cracks, the overall integrity of the wall had not changed significantly. Less cracks were noted in tubes that were incubated for less time, indicating that crack formation was cumulative and additional cracking upon drying of the tubes was not observed, ruling out the likelihood of a significant drying effect [27,28].

The macroscopic pattern obtained was rationalized as stress-related cracking, given the physico-chemical nature of injection-molded polypropylene and the shape and orientation of the cracks. The cracking appeared to require chemical initiation and was likely governed by the micromorphology of the skin layer and associated anisotropic stresses. Similar patterning had been observed in heated, weathered and laboratory irradiated samples [29, 30].

All tubes modified using the different oxidation methods showed the same macroscopic cracking effect. Tubes which were modified under mixing conditions showed slightly less cracking.

Further investigations were made using scanning electron microscopy (SEM) methods to examine the topological properties of the reacted surfaces. By this method, the depth of crack formation was observed along the broken edges of a sample. The crack depth was variable and estimated to be in the order of $20\mu\text{m}$ (Figure 26).

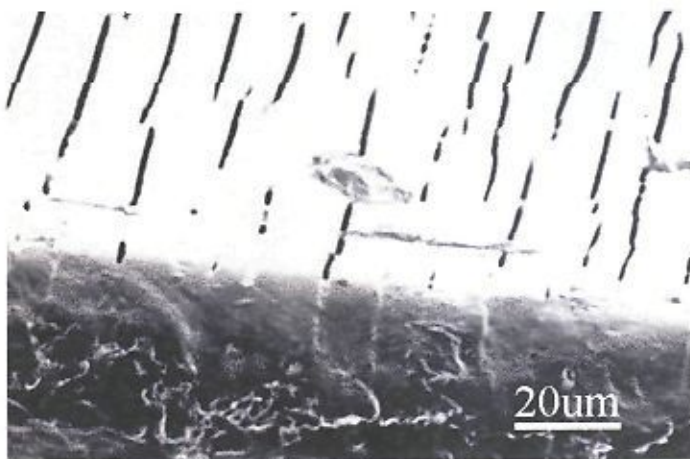


Figure 26: SEM micrograph of APS-treated, oven-heated tube taken from the cross-sectional viewpoint but tilted slightly towards the inner face.

Using higher magnifications, a spaghetti-like mesoscopic topology was noted that was reminiscent of the microvilli in brush border membranes (Figure 27).

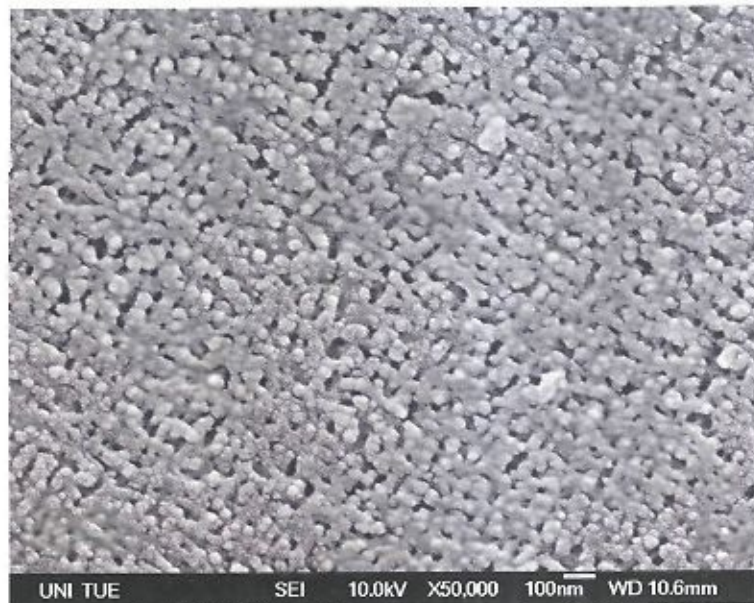


Figure 27: SEM micrograph of APS-treated, oven-heated surface showing mesoscopic spaghetti-patterning on the inner face.

In contrast, the sulfate-treated control surface remained smooth (Figure 29). Also, a gain of surface area of an order of magnitude was estimated by contrasting the image following oxidation (Figure 30) against that of an untreated control surface (Figure 28).

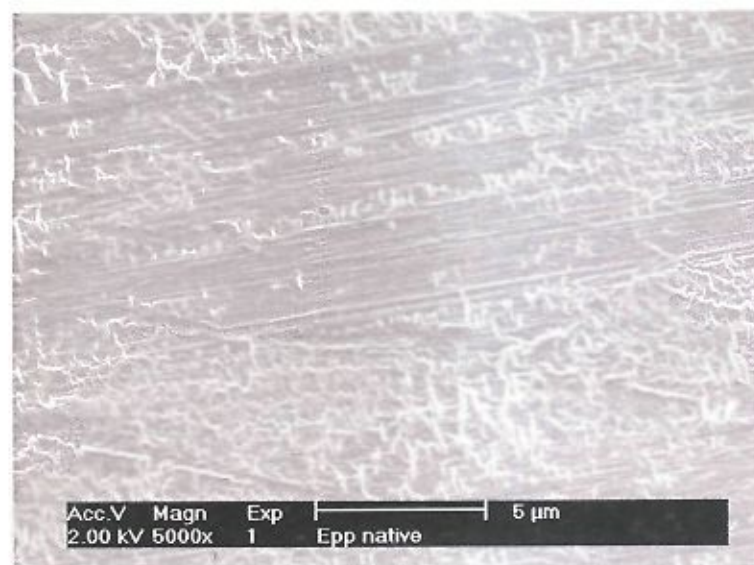


Figure 28: SEM micrograph of native Eppendorf Tube surface.

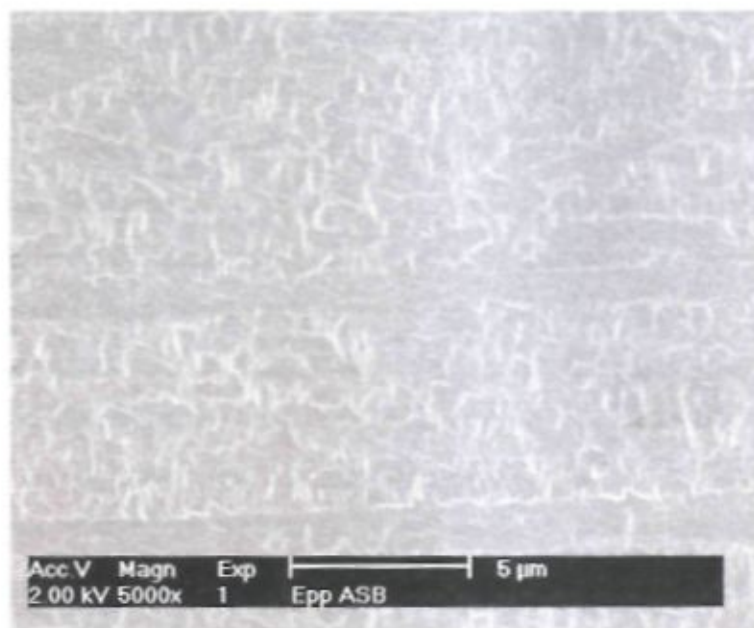


Figure 29: SEM micrograph of sulfate-mediated surface treated in oven.

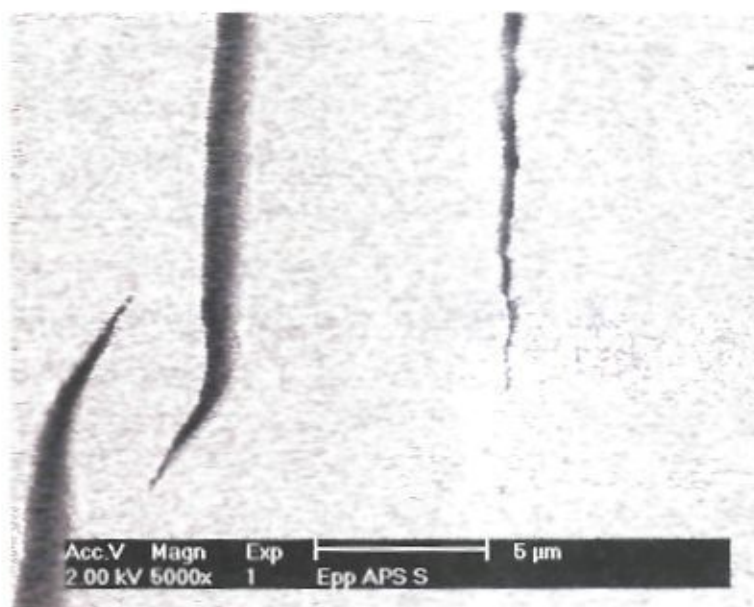


Figure 30: SEM micrograph of APS treated surface modified in oven

Cross-sectional views obtained at higher power resolution (results not shown) could not discern the base position of the spaghetti pattern, but the depth of penetration was estimated from the image to be on the order of 300nm.

The seemingly chaotic patterning in fact displayed elements of regularity. For example, the individual tentacles or "spaghetti" pieces had the same approximate diameter and separation. This appearance initially suggested that the persulfate reagent had commenced attack preferentially at amorphous regions of the polymer residing within the topmost regions of the skin layer. Upon reconsideration, however, it appeared that a patterning of this regularity may have been created by oscillation of oxidation reaction. Oscillation may occur whenever the equilibrium of individual steps of an overall chemical process is shifted, usually by temperature. The shift can be more dramatic if the supply and removal of chemical species is diffusion limited because diffusion coefficients are less sensitive to temperature effects than are those of typical chemical processes. It follows that under the appropriate experimental conditions, reagent access to a surface site and product removal from that site could spatially and temporally mediate a process, thereby affording a pattern [31].

With respect to the free radical-promoted oxidation of polypropylene, the possibility of a chemical oscillation and consequential patterning of the surface was considered in view of the fact that stirring was not employed during the oven modification and a diffusional constraint, namely, a surface, described part of the reaction system. BET surface area estimates were attempted of crushed tubes pooled together, however, the samples prepared nevertheless demanded detection at threshold levels and their measurements proved irreproducible.

Speedvac modified surfaces showed the same topological properties like the oven modified surfaces with respect to a slight decrease of the density of the mesoscopic patterning (Figure 31). This decrease is based on vibrations of the speedvac during the modification caused by mild centrifugation. This vibration was interpreted as a kind of mild mixing, which disturbs the diffusion system of the reaction and the chemical oscillation, resulting in a less patterned surface [31]. In contrast, micrographs of the

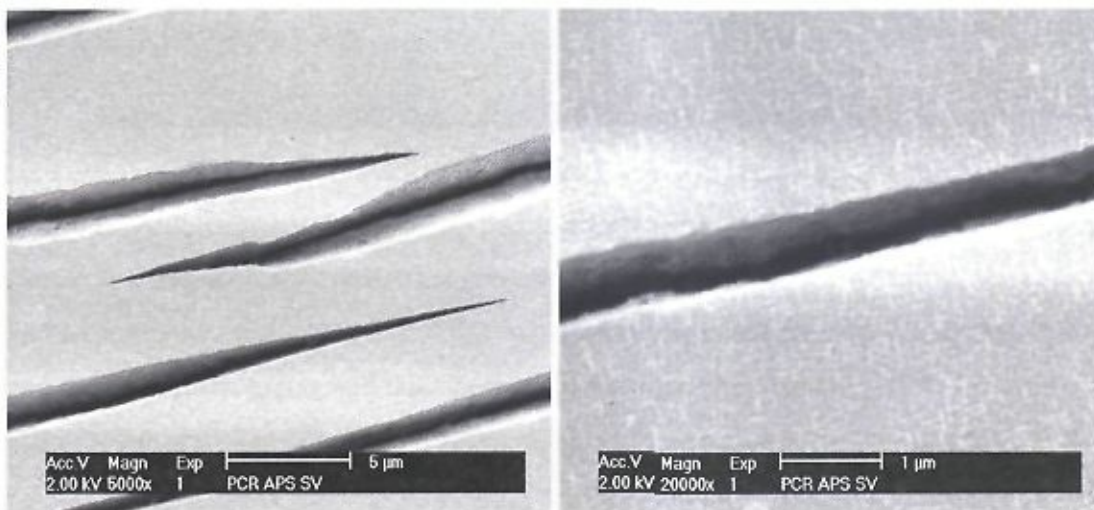


Figure 31: SEM micrographs of APS treated surfaces modified in speedvac.

surfaces modified by thermomixer oxidation methods indicated that the mesoscopic patterning was lost. During this kind of modification tubes were constantly mixed, resulting in a drastic loss of the chemical oscillation of the system. With the loss of this reaction-diffusion system, no chemical oscillation could take place and no mesoscopic patterning was noted (Figure 32). Current efforts are focused on validating the basis of the patterning,

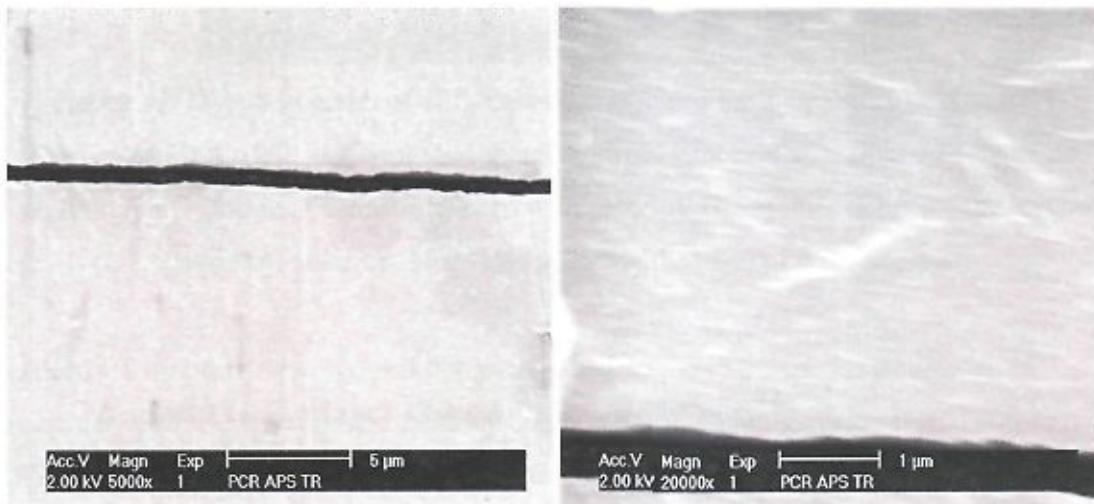
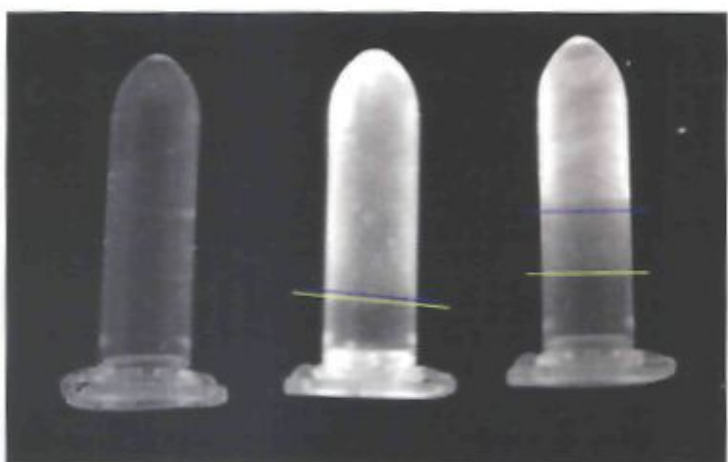


Figure 32: SEM micrographs of APS treated surfaces modified in thermomixer.

elucidating any variations in functional group composition along the surface, and exploiting any regional differences of physico-chemical features, such as wettability.

metabolites. The spectra also showed thin protein had bound to the oxidized surfaces. In particular, characteristic amide stretching bonds were noted in the region from 1600–1650cm⁻¹ (results not shown) [32]. The surface chosen for protein binding studies bore

Figure 33: UV-photograph of different surfaces tested for their ability to bind trace-dansylated BSA. (left: static tube incubated with protein; center: shaken tube incubated with protein; right: native tube incubated with protein). Green lines delineate the level of dansylated BSA. Blue lines delineate the level of fluorescence.



Surfaces of the modified Eppendorf tubes, oxidized using oven, speedvac and thermomixer methods, were tested for their ability to bind IgG. After an incubation period during which protein and surface were allowed to interact, the tubes were washed as previously discussed. Photographs were taken under UV-light to view any binding along the inner surfaces. Images taken directly after the incubation indicated that only oxidized surfaces retained fluorescent protein (Figure 33). Native surfaces did not retain protein to a significant degree. Protein binding was also monitored using ATR-FTIR

(vi) Protein Immobilization

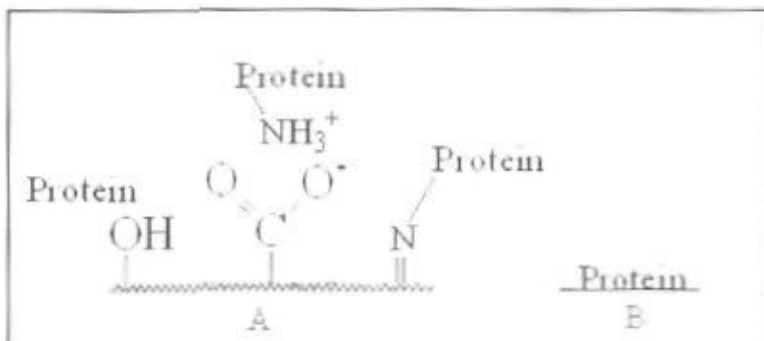


Figure 34: Possible modes of protein binding to oxidized polypropylene.

an assortment of hydroxyl carboxylic acid and ketone functions. The hydroxyl and carboxylic acid groups interact with polar residues on the protein and achieve binding via H-bonding and dipole-dipole interactions. Carboxylic acid groups in addition can form salt bridges with protein amino groups (Figure 34:A) [33-35]. Further, protein amino groups can form imines with ketones. In this case presumably, imine formation with protein ammino groups leads to protein immobilization, although the imine formation is reversible [36].

While the increase of binding was undeniable due in part to an increase of surface area, the chemical nature of the surface-protein interaction was also important to consider. In case of native tubes, the binding process is due to hydrophobic-hydrophobic interactions. In the case of oxidized tubes, however, the binding process is presumably dominated by polar interactions [33-35].

Washing of the surfaces showed that the proteins were not adsorbed permanently and were able to leach off during the washing procedures. Proteins were usually retained during the high-salt washings but could be removed during the low-salt washings (Figure 35).



Figure 35: Photograph series illustrating three tubes incubated with protein (leftmost: protein incubated with shaking; center: protein incubated without shaking; rightmost: oxidized tube not applied to protein incubation) and washed in parallel fashion (left picture: after removing excess protein solution; center picture: washing briefly with water; right picture: after washing 5min more with water).

Differences in protein adsorption between oxidized surfaces that were modified using different methods could be noted. Oxidized surfaces afforded by the speedvac modification released adsorbed protein slightly faster (not shown) than surfaces modified in the oven. Surfaces modified by thermomixer methods released the adsorbed proteins most rapidly, within the first washing. These results strongly suggest that the mesoscopic patterning of the surfaces had a great influence on protein adsorption. Surfaces with undulating patterns bound and retained protein in higher yields than surfaces with little or no mesoscopic patterning.

2.4 Conclusion

Oxidation of Eppendorf Safe-Lock tubes was realized using three methods in which concentration and reaction-diffusion parameters were varied. Contrasting topologies were afforded as a result. In each case, inert surfaces were chemically activated to bear surface-pendant functional groups and the surface area was increased to different extents by a macroscopic and mesoscopic patterning. These new surface properties introduced the possibility of enhanced protein immobilization on the surfaces. While macroscopic patterning was consistent, the mesoscopic patterning and degree of protein binding could be controlled using different methods of modification.

2.5 Acknowledgements

M.K. thanks Alpay Taralp, Mehmet Ali Gülgün, Istem Özen, Kazim Acatay and Arzu Altay of Sabancı University for very helpful suggestions and assistance.

SEM analyses were performed by Dorothea Adam and Döne Demirgöz of the University of Tübingen, Institute of Applied Physics, and by David Milius and Daniel Dabbs of Princeton University, SEM facility.

2.6 References

- [1] J. Karger-Kocsis, *Polypropylene: An A-Z reference*, Kluwer academic Publishers, London, 1999
- [2] Ser van der Ven, *Polypropylene and other Polyolefins, Polymerization and Characterization*, Elsevier, 1990
- [3] S. V. Meille, α - γ -Disorder in Isotactic Polypropylene, *Crystallized und High Pressure*, Marcomolecules, 29, 1996
- [4] G. Kalay, M. J. Bevis, *Preocessing and Physical Property Relationships in Injection-molded Isotactic Polypropylene: 2. Morphology and Crystallinity*, J. o. Polymer Science, 35, 1997
- [5] K. Cho, D. N. Saheb, J. Choi, H. Yang, Real time *in situ* X-ray diffraction studies on the melting memory effect in the crystallization of β -isotactic PP, *Polymer*, 43 (4), 2002
- [6] A. Kron, B. Stenberg and T. Reitberger, *Characterisation of polypropylene peroxides; their thermo-oxidative stability and reactivity towards dimethylsulfide*, *Polymer Degradation and Stability*, 54 (1), 1996
- [7] *The Aldrich Library of FT-IR Spectra*, Edition II, Sigma-Aldrich Co., 1997.
- [8] M. Hesse, H. Meier, B. Zeeh, *Organic Spectroscopy, Methods and Applications*, Thieme, Stuttgart, 1997
- [9] D. Lin-Vien, N. B. Colthup, W. G. Fateley, J. G. Grasselli, *The Handbook of Infrared and Raman:Characteristic Frequencies of organic Molecules*, Academic Press, 1991
- [10] Zhikang Xu, et al., *Microporous Polypropylene Hollow Fiber Membrane, Part I, Surface Modification by the Graft Polymerization of Acrylic Acid*, J. O. Membrane Science, 196, 2002
- [11] J. C. Philippart, F. Posada, J. L. Gardette, *Mass Spectroscopy Analysis of VoLatile Photoproducts in Photooxidation of PP*, *Polymer Degradation and Stability*, 49, 1995
- [12] L. Achimsky , L. Audouin , J. Verdu, *Kinetic study of the thermal oxidation of polypropylene*, *Polymer Degradation and Stability*, 57, 1997
- [13] S. Commereuc, D. Vaillant, J. L. Philippart, J. Lacoste, J. Lemaire, D. J. Carlsson, *Photo and thermal decomposition of iPP hydroperoxides*, *Polymer Degradation and Stability*, 57, 1997

- [14] C. H. Bamford, K. G. Al-Lamee, *Studies in polymer surface modification and grafting for biomedical uses: 2. Application to artierial blood filters and oxygenators*, Polymer, 37 (22), 1996
- [15] F. Gugumus, *Re-examination of the thermal oxidation reactions of polymers 3. Various reactions in polyethylene and polypropylene*, Polymer Degradation and Stability, 77, 2002
- [16] J. M. Garcia-Martinez, O. Laguna, S. Areso, and E. P. Collar, *FTIR Quantitative Characterization of Chemically Modified Polypropylenes Containing SuccinicGrafted Groups*, Polymer Degradation and Stability, 73 (14), 1999
- [17] A. Tidjani , Y. Watanabe, *Comparison of polyethylene hydroperoxide decomposition under natural and accelerated conditions*, Polymer Degradation and Stability, 49, 1995
- [18] P. Gijsman, J. Hennekens, J. Vincent, *The influence of temperature and catalyst residues on the degradation of unstabilized polypropylene*, Polymer Degradation and Stability, 42, 1993
- [19] D. J. Carlsson, D. M. Wiles, *The photodegradation of polypropylene films. II. Photolysis of ketonic oxidation products*, Macromolecules, 2, 1969
- [20] J. Rychlý, C. Matisová-Rychlá, D. Juréčk, *Chemiluminescence from Oxidized Polypropylene During Temperature Cylcling*, Polymer Degradation and Stability, 68, 2000
- [21] Jun-Ichiro Hayashi, Takeshi Nakahara, Katsuhi Husahabc, Shigejarn Morooka, *Pyrolysisof Polypropylene in the Presence of Oxygen*, Fuel Processing Technology, 55, 1998
- [22] F. Gugumus, *Thermolysis of Polyethylene Hydroperoxides in theMelt, 5. Mechanisms and Formal Kinetics of Product Formation*, Polymer Degradation and Stability, 76, 2002
- [23] F. Gugumus, *Contribution to the Role of Aldehydes and Peracids in Polyolefin Oxidation, I. Photolysis and Photooxidation of Aldehydes in Polyethylene*, Polymer Degradation and Stability, 65, 1999
- [24] F. Gugumus, *Thermooxidative degradation of polyolefins in the solid state-6. Kinetics of thermal oxidation of polypropylene*, Polymer Degradation and Stability, 62, 1998
- [25] S. Girois, P. Delprat, L. Audouin, J. Verdu, *Oxidation thickness profiles during photooxidation of non-photostabilized polypropylene.*, Polymer Degradation and Stability, 56, 1997

- [26] S. Girois, P. Delprat, L. Audouin, J. Verdu, P. Delprat, G. Marot, *Molecular weight changes during the photooxidation of isotactic polypropylene*, Polymer Degradation and Stability, 51, 1996
- [27] A. P. Parker, The mechanics of fracture and fatigue: An introduction, E. & F.N. Spon Ltd., NY, 1981.
- [28] A. A. Griffith, *VI. The phenomena of rupture and flow in solids. Philosophical Transactions of the Royal Society of London Series A* 1921:221
- [29] G. G. Chell, *Developments in fracture mechanics – I: Development series*, Applied Science Publishers Ltd. Essex, England, 1979
- [30] A. O. Ibhadon, *Fracture Mechanics of Polypropylene, Effect of Molecular characteristics, crystallisation and annealing on morphology and impact performance*, Journal of Applied Polymer Science, 69, 1998
- [31] L. Yang, M. Dolnik, A. M. Zhatotinsky, I. R. Epstein, *Spatial resonances and superposition patterns in a reaction-diffusion model with interacting turing modes*, Physical Review Letters 2002; 88:208303-1 – 208303-4
- [32] E Brynda, M. Houska, J Škvor, J. J. Ramsden, *Immobilization of Multilayer Bioreceptor Assemblies on Solid Substrates*, Biosensors & Bioelectronics, 13 (2), 1998
- [33] J.-Y. Yoon, J.-H. Kim, W.-S. Kim, *Interpretation of protein adsorption phenomena onto functional microspheres*, Colloids and Surfaces B, 12, 1998
- [34] J.-H. Kim, J.-Y. Yoon, *Encyclopedia of Surface and Colloid Science*, 2002
- [35] S. Semal, T. D. Blake, V. Geskin, M. J. de Ruijter, G. Castelein, J. De Coninck, *Influence of surface roughness on wetting dynamic*, Langmuir, 15, 1999
- [36] J. March, *Advanced organic chemistry, 3rd edition*, John Wiley and Sons, 1985

Chapter 3: Second Generation Surfaces: Oxidized PP Coated Using TEOS

3.1 Introduction

The Surface chemistry of polypropylene oxidation was developed in the previous chapter. In particular, results therein indicated that oxidized surfaces were conveniently realized. Also, results indicated the tubes bound more protein in proceeding from native to oxidized state. This increase in binding was presumably afforded by surface-pendant functional groups, which included alcohols, carboxylic acids and possibly ethers and esters, as well as by an increased overall surface area. More importantly, the modification afforded activated surfaces for potential use in various applications. That being said, the strategy using persulfate oxidation was limited in the number of different surface-pendant functional groups that would be afforded. Considering this fact, the strategy of the oxidation was not only used to produce reactive surfaces in this study, but also to form an intermediate foundation with the ability to readily-bond other chemical components, resulting in coatings of much greater diversity. The advantage of realizing diversity in coatings is that it introduces the ability to address a multitude of possible applications based in rational choice of surface groups, compared with the finite functionalities available in oxidized surfaces.

To test the potential of the oxidized surfaces, the condensation products of tetraethoxysilane (TEOS) were coated thereon, affording high area, pre-glass-like surfaces.

Surfaces featuring silicon dioxide glasses are generally used in the form of silica beads or well-plates for achieving DNA and mRNA purification in the life-sciences. These commercially available surfaces are usually sold exclusively in kits, combined with the necessary chemicals. The surfaces are usually difficult to purchase separately and are offered like the kits, at considerable expense, presumably due to patent constraints.

The advantage of the herein introduced “silica” coated tubes is that they offer the same abilities like the commercial analogs, but can be easily produced in any laboratory without using any special chemicals or high expense equipment. Another advantage is, that

the coated tubes can be prepared on demand or be stored for extended periods. Considering these facts, namely, that the surfaces are coated on the inside of standard tubes, easily handled, and precluding of the need of additional laboratory equipment, the concept examined in this chapter bears noteworthy advantages compared to commercial glass-based packing materials. Most importantly, the technology presented herein is patentable, as current patents cover designs and packing materials, but not any "coated-tube" technologies.

3.2 Materials and Methods

Silanes, Chemicals, Proteins and Kits

Tetraethoxysilane (TEOS) was purchased from United Chemical Technologies (UCT) Inc. Bovine serum albumin (BSA) and 5-dimethylamino-1-naphthalenesulphonyl chloride (dansyl chloride) were obtained from Sigma-Aldrich Laborchemikalien GmbH. Dialysis bags (3500 molecular weight cut-off) were obtained from Pharmacia. Total mRNA-extraction and mRNA-purification kits were supplied from QIAGEN. Deionized water ($18\text{M}\Omega/\text{cm}^3$) was produced in-house using a Millipore Academic system. Reagent grade solvents were obtained from commercial suppliers.

3.2.1 General Methods (GM)

(i) Preparation of Silane Solutions

Solutions of tetraethoxysilane (TEOS) of the composition organosilane/*i*-propanol (1:94) were prepared in Falcon Tubes (50ml). After the mixture was agitated well using a VELP brand vortex, water (5%) was added to initiate the condensation reaction. These solutions were incubated (15min, RT) affording the intermediate condensation products of TEOS. The TEOS solutions were freshly prepared before each experiment to maintain consistency of the condensed products.

(ii) Washing and Drying of Coated Surfaces

Following incubation, the reaction solutions were removed from the tubes using a pipette. Residing solutions were centrifuged using an Eppendorf brand micro-centrifuge (13200rpm, 1min) and subsequently removed. To wash the inner surfaces, the tubes were

filled with *i*-propanol. After withdrawing the washing solutions the tubes were dried *in vacuo* (70°C, 2h). To remove adsorbed but not immobilized reagent, as well as to assure the total hydrolysis of residual ethoxysilanol bonds leading to maximum crosslinking of immobilized reagent, the tubes were once filled with water to the top. After the water was removed with the aid of a pipette, the tubes were dried again *in vacuo* (70°C, 2h).

(iii) Preparation and ATR-FTIR Analysis of Eppendorf Tubes

Eppendorf Tubes were prepared in a way that would permit effective analysis using the attenuated total reflectance (ATR) accessory of the FTIR instrument. As excessive bending of samples during the sample preparation yielded poor ATR-FTIR spectra, this modification to the method was introduced to protect the crystal structure of the polymer. A cylindrical piece with an approximate height of 3mm was cut from a region just above the hemispherical base of the tube using a razor blade heated in a Bunsen burner. The cylindrical ring was frozen in liquid nitrogen and shattered into small pieces with approximate dimensions of 2x3mm. These pieces were then *in vacuo* (40°C, 2h). Samples prepared in this way had little or no damage to the crystal structure but nevertheless some bore thick edges, which arose from the cutting action of the hot blade. These regions were carefully exercised with a flat-edged razor blade. The samples were tightly fixed over the measurement window of the ATR accessory of a Bruker model Equinox 55 infrared spectrophotometer. Twenty scans were averaged and displayed using rubber-band correction at 70 points in the Bruker OPUS V3.1 software of the system.

(iv) Trace Dansylation of Bovine Serum Albumin (BSA)

Heat-shock fractionated BSA (100mg) was dissolved in water (10ml) and the pH value was adjusted to 9 using sodium hydroxide solution (1M). 5-Dimethylamino-1-naphthalenesulfonyl chloride (Dansyl chloride, 5mg) was dissolved in acetonitrile (100µl) and slowly added to the gently stirring BSA solution maintaining the pH value between 8 and 9 using sodium hydroxide solution. After 1h, the solution was delivered into a dialysis

bag and dialyzed (25°C) against 3x4L water. Ninhydrin color analysis of native albumin and dansylated albumin indicated that at most 10% of the amino groups had been transformed into the sulfonamide fluorophore. The dansylated protein was stored at 4°C.

(v) Immobilization Method for Trace Dansylated Protein UV Analyses

A portion of the dansylated BSA stock was added to excess salt solution (1M NaCl) in order to afford a dilute stock (0.3mg protein/ml, pH 7) that would be appropriate for immobilization studies. This solution was transferred in the modified tubes and incubated (37°C, 1.5h). The solution was withdrawn, and the residing liquid was pooled by centrifugation and collected using a pipette. Photographs were obtained using an Uvitec UV-box with an Ihi CCD camera mounted. The tubes were filled with aqueous sodium chloride solution (1M, 1ml) and agitated (2min). The washing solution was withdrawn and the tubes were again photographed. Next, the tubes were washed with water and similarly documented. After that, the same washings were performed with 10% Triton X100 and 10% NP-40 solutions. Photographs were taken after every washing.

3.2.2 Second Generation TEOS Coating Procedure

Previously oxidized Eppendorf Tubes were incubated (RT, 1.5h) with freshly prepared activated TEOS solutions (1.5ml). After reaction, the tubes were washed and dried as described previously (GM). Samples were prepared using standard procedures (GM) and examined using ATR-FTIR analysis. Additionally, the swelling properties of TEOS-coated tubes were crosschecked against native tubes by incubating toluene in native and coated tubes (1ml, 70°C, 2h). To examine the ability of the silica coated surfaces to bind protein, immobilization studies using trace dansylated BSA were carried out.

3.2.3 Life-Science Application of TEOS-Coated Surfaces: mRNA Purification

Eppendorf Tubes were oxidized and coated using TEOS with the intention to perform mRNA purification out of total RNA. Two different coating methods were tested. The purification was carried out using established QIAGEN protocols and QIAGEN reaction solutions. The mRNA purification using TEOS-coated tubes was validated and quality-checked against a parallel purification using the QIAGEN Oligotex Spin Column.

(i) Preparation of Oxidized Surfaces for mRNA Purification

Eppendorf Tubes filled with APS solutions (1M, 1.5ml) were fixed in an oven as discussed before and incubated (70°C, 24h). Following reaction, the solutions were discarded, and tubes were rinsed with water and dried (70°C, 16h).

(ii) TEOS Coating Procedures for mRNA Purification

TEOS solutions (A and B) were freshly prepared. Solution A had a composition of TEOS/H₂O/*i*-propanol (1:10:189) and solution B had a composition of TEOS/Et₃N/H₂O/*i*-propanol (1:2:10:187). These stocks were preactivated (RT, 10min) and delivered into the previously oxidized Eppendorf Tubes. Following incubation (1ml, RT, 30min), solutions were withdrawn and the tubes were agitated with *i*-propanol (2.5ml). The solvent was removed using a pipette, and the tubes were inverted (4min) and dried as such in an oven (40°C, 28h). A final rinse with water and drying step (40°C, 20h) was performed.

(iii) Isolation of Total RNA

Plant material (*Triticum durum*, 100mg) was pulverized in an RNase-free, liquid-nitrogen cooled mortar. The material was immediately transferred into an RNase-free,

liquid-nitrogen cooled 2ml capacity Eppendorf Tube. RLT Buffer (450 μ l) was added onto the plant powder and the suspension was vortexed. Sample was incubated (3min, 56°C) to ensure better tissue disruption. The lysate was transferred into a QIA Shredder Spin Column placed in a 2ml capacity collection tube and centrifuged (14,000rpm, 2min). Supernatant was carefully transferred into a fresh RNase-free tube without disturbing the cell debris at the bottom of the Eppendorf Tube. One half volume of ethanol was added to the clear solution. The liquid was mixed by the gentle, oscillating push-release action of a pipette. A sample was delivered into an RNeasy Mini Column placed in a 2ml capacity collection tube. The column was centrifuged (10,000rpm, 30s) and the flow-through was discarded. The remainder of the sample was applied into the same column and the centrifugation procedure was repeated. RW1 Buffer (700 μ l) was added to the RNeasy Column and centrifuged (10,000rpm, 30s). The flow-through and the collection tube were discarded. The column was transferred into a collection tube. RPE Buffer (500 μ l) was added into the column. The column was centrifuged (10,000rpm, 30s). The flow-through was discarded. The previous step using RPE buffer was repeated but this time centrifugation was extended (2min). To elute the total RNA, the contents of the column were placed into a new RNase-free 1.5ml capacity Eppendorf Tube. RNase-free water (50 μ l) was placed directly onto the silica membrane and incubated (1min, RT). The column then was centrifuged (10,000rpm, 1min) to elute total RNA. The collected total RNA sample was quantified spectrophotically ($A_{260} = 1 \rightarrow 40 \mu\text{g/ml}$) and visualized and validated on an agarose gel.

(iv) mRNA Isolation from Total RNA

The Total RNA solution was divided equally and one half was processed in the QIAGEN Oligotex Spin Column while the other was processed in the surface-modified, 2ml capacity Eppendorf Tubes.

Purification Following Established QIAGEN Protocol

Oligotex suspension was ramped to 37°C in a heating block, vortexed and stored (RT). In the meanwhile, the sample was topped off with RNase-free water to the 250µl mark and an equal volume of OBB Buffer (250µl) was added. The Oligotex suspension (15µl) was carefully delivered into the tube. The contents were mixed by gently flicking the tube. The sample was incubated (3min, 70°C) to impede/disrupt any possible RNA secondary structures. The sample was incubated (10min, RT) to permit hybridization. The sample and Oligotex was centrifuged (14,000rpm, 2min) and the supernatant was carefully removed. The pellet was resuspended in OW2 Buffer (400µl) by the gentle, oscillating push-release action of a pipette and the contents were transferred into a small spin column. Following centrifugation (14,000rpm, 1min), the column was placed into an RNase-free 1.5ml Eppendorf Tube, and OW2 buffer was added (400µl). The sample was centrifuged (14,000rpm, 1min) and the flow-through was discarded. The spin column was transferred into a new RNase-free 1.5 ml Eppendorf tube. Hot OEB Buffer (50µl, 70°C) was added to the column and the resin was resuspended by the gentle, oscillating push-release action of a pipette. The column was centrifuged (14,000rpm, 1min). Hot OEB buffer was added twice again to maximize the yield of mRNA.

Purification Using TEOS-Coated Tubes

The sample was transferred into a TEOS-coated tube and topped off with sterile, RNase-free distilled water up to the 250µl mark. An equal volume of buffer (250µl) was delivered into the column. The sample was incubated (3min, 70°C) to impede/disrupt any possible RNA secondary structures. The sample was incubated (20min, RT) in a shaker to permit hybridization. The tube was washed with OW2Buffer (500µl). mRNA was eluted by exposing all accessible surfaces with OEB Buffer (100µl). Water was also used successfully in place of elution buffer.

(v) Amplification and Analysis of Purified mRNA

The target mRNA was amplified using standard reverse-transcriptase polymerase-chain reactions in an Eppendorf brand Thermocycler. Withdrawn samples were migrated in an agarose gel (1.5wt%, 100V, 45min) inoculated with ethidium bromide. The gel was photographed using an Uvitec model Biolab CCD camer equipped UV-box (254nm, 320ms integration time).

3.3 Results and Discussion

(i) TEOS Coating

Previously oxidized Eppendorf Tubes were reacted with solutions of TEOS, affording the 2nd generation TEOS coating. The coating reaction was monitored using ATR-FTIR spectroscopy. The discussion herein is based on the results of these measurements and on basic organo-silane chemistry.

The TEOS coating is presumed to occur by a multistep-reaction (Figure 36). The first step of the reaction, initiation, was performed by adding water to the TEOS-*i*-propanol solution. TEOS was hydrolyzed, affording the hydrolysis products and ethanol (A). The hydrolysis products rapidly followed a dimerization pathway via intramolecular condensation, with concomitant loss of water, affording an oligomeric network between the hydrolyzed TEOS molecules (B). It is noteworthy that hydrolysis and condensation of TEOS overlap. By the principle of chemisorption, dimers shown in the diagram dock onto surface-pendant hydroxyl groups via hydrogen-bonding interactions (C).

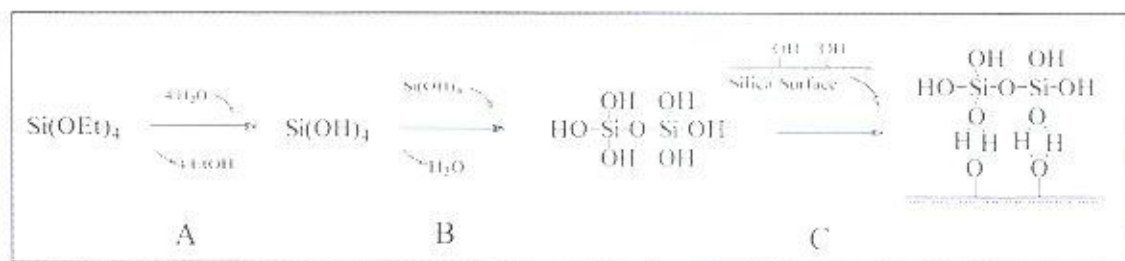


Figure 36: Hydrolysis, dimerization and chemisorption of TEOS

Finally the hydrogen bonds transform into covalent bonds via condensation induced by heat (Figure 37:D) [1, 2].

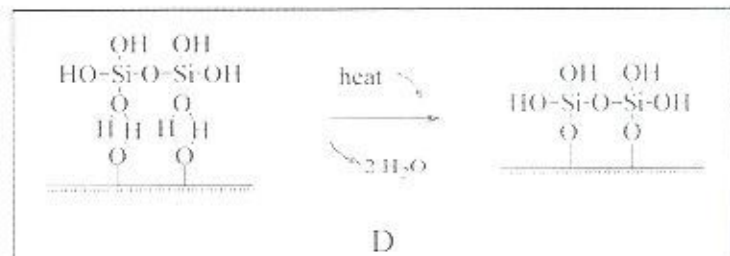


Figure 37: Condensation of TEOS hydrolysis products

This process normally does not a monolayer coating. By repetition of the first reaction steps (A-C), multilayers of silanes can build up, typically forming 5-15 layers in typical deposition protocols. Curing (D) accordingly afford a multilayer coating of TEOS on the surface of the oxidized tubes [3].

The ATR-FTIR spectra pointed out, that the tubes reacted with TEOS solutions showed a low, but significant change in the lower fingerprint region ($1200\text{-}800\text{cm}^{-1}$) (Figure 38) that was consistent with the Si-O stretch of siloxanes. In light of the threshold sensitivity of the ATR unit, it followed that a multilayer must have been formed as anticipated. Therefore this spectral data validates a successful coating. Changes in

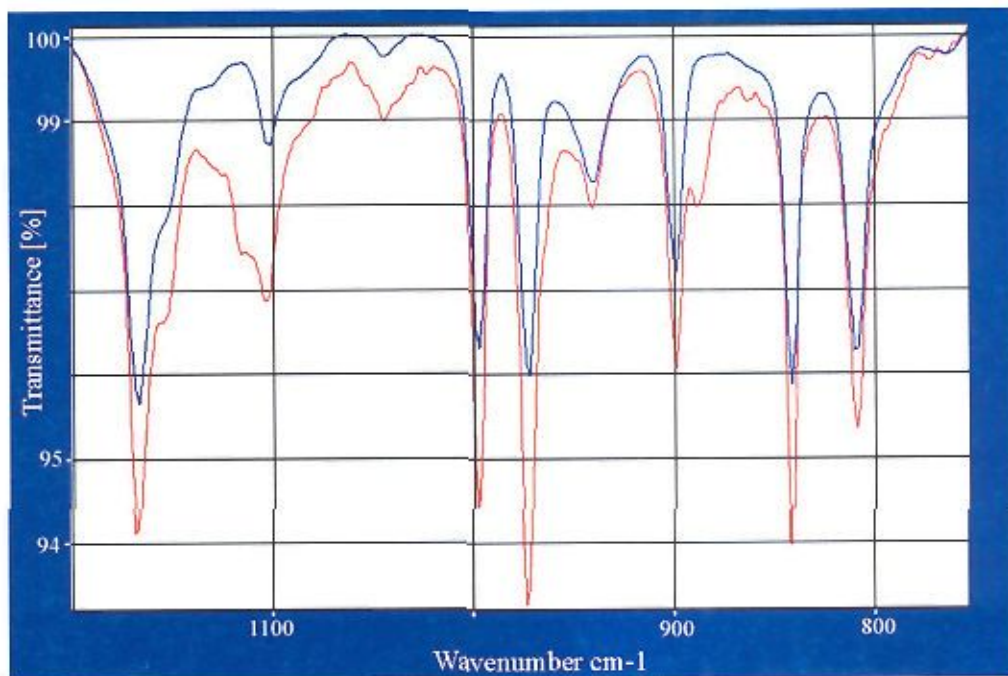


Figure 38: ATR-FTIR spectra of oxidized (blue) and TEOS-coated (red) polypropylene surfaces

surface bonding were only observed in the lower fingerprint region. The result was encouraging, as ketones and carboxylic acids should not have reacted with the silanes during the coating process. Only surface hydroxyl groups should have reacted with the silanes, however, no change was anticipated nor observed in the high-frequency region ($4500\text{-}3000\text{cm}^{-1}$) as the silane-surface offered the same equivalent of silane-bound hydroxyl groups like the oxidized surface. Upon further consideration it was noted at any rate that the ATR accessory was incapable of examining only the surface-pendant hydroxyl groups due to sensitivity considerations. A peak for the Si–O–C stretching, centered at 1115cm^{-1} and the peak at 889cm^{-1} which corresponded to non-binding oxygen sites in the silica network confirmed a successful coating [4 - 6].

Swelling experiments implemented by incubation of toluene in the TEOS-coated tubes validated the presence of silica multilayers coating the inner surface of oxidized Eppendorf Tubes. While native and oxidized tubes afforded longitudinal expansion during the toluene incubation, TEOS-coated oxidized tubes afforded no significant

changes in the dimensional properties. This observation suggested, that the surfaces of the oxidized tubes were completely coated with a pre-glass layer, which was impermeable to solvent.

(ii) Protein Immobilization

Trace-dansylated BSA was immobilized on the TEOS-coated surfaces during the studies. Like the organic surfaces, protein adsorbed during the incubation was retained in the beginning on the coated surfaces. However, washing experiments pointed out that the protein was not permanently bond. Adsorbed protein was able to be washed off during the first washing using high-salt solution. Last remains of fluorescent protein were totally removed by the second washing using water (Figure 39). Fluorescence remaining on the coated surface corresponded to self-fluorescence.

Protein binding studies on porous glass have shown that optimal retention occurs when the protein size is a little under the pore size of the matrix [7]. This finding suggests that the TEOS coating filled the grooves of the mesoscopic topology, possibly affording a much flatter surface.

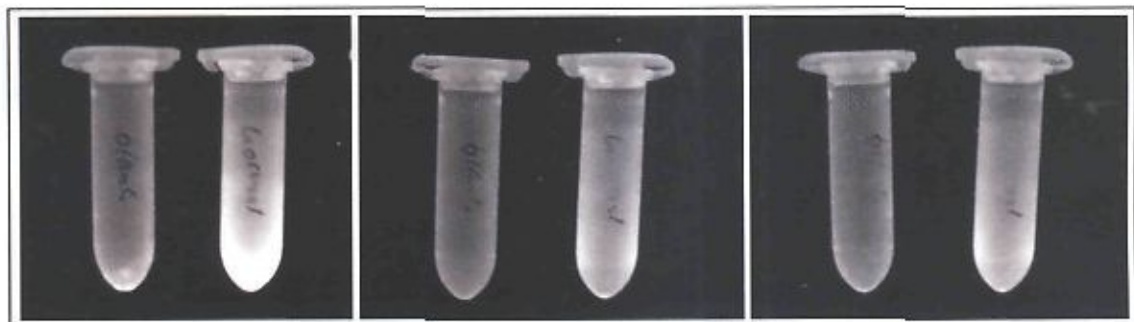


Figure 39: UV-photographs of protein immobilized on native surfaces (left) and TEOS-coated surfaces (right).

(right: unwashed; center: agitated with high salt; right: agitated with water)

TEOS-coated surfaces retained protein less effectively than the oxidized surfaces. Clearly, the coating affected the chemistry and the physico-chemical properties of the surface. In contrast to the oxidized surfaces, TEOS-coated surfaces bear only hydroxyl groups, pendant to the silica coating, as moieties available for protein binding. Surface-pendant alcohols, carboxylic acids and ketones were not chemically attended during the coating procedures. These reactive groups were no longer accessible for protein binding interactions, as they were covered by the silica multilayer. Considering this fact, protein binding in the example of TEOS-coated tubes was only governed by hydrogen-bonding (Figure 41:A) and adsorption effects Along the new surface (Figure 40:B) [1, 2, 8].

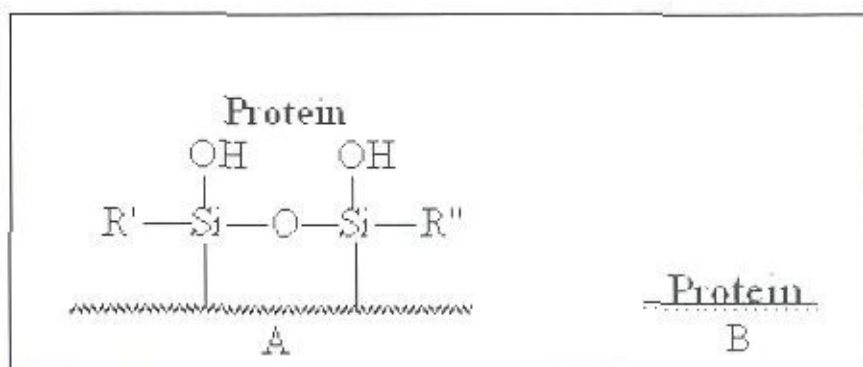


Figure 40: Plausible protein binding modes for TEOS-coated surfaces

Protein immobilization results indicated that TEOS-coated surfaces could not be used to bind protein permanently, but showed potential for possible application as temporary carrier material for biomolecules.

(iii) mRNA Purification

Following established QIAGEN protocols, mRNA purification was performed using TEOS-coated surfaces afforded by two different coating procedures. One coating of the oxidized tubes was performed using the standard coating procedures, the second coating was performed with 1% triethylamine added as catalyst.

While the purification using a standard QIAGEN Spin Column (control) proved to be a complex five-step procedure, the mRNA was purified using a simplified two-step procedure based on TEOS-coated tubes. The UV-analyses point out that organic material with an approximate size of 250 base pairs, was extracted out of the Total RNA (Figure 41). The result matched the base pair sizes of the material extracted by the QIAGEN Spin Column (result not shown), which indicated that mRNA was successfully purified out of Total mRNA using TEOS-coated surfaces.



Figure 41: Electrophoresis results of the mRNA purification visualized under UV-light

While the ATR-FTIR spectral data from the two TEOS methods differed (results not shown) no effect of this difference between the surfaces was reflected in the purification. This indicated that catalyst-activation need not to be used during the chemical coating reactions, in contrast to typical sol-gel processes [9]. Quantitative experiments using Real-Time-PCR procedures were not performed in this study, but will form the basis of continuing investigations. Considering the fact that modified tubes of 2.0ml capacity had proven slightly inconvenient for applications on the microliter-scale, parallel investigations using Eppendorf PCR Tubes of 0.2ml capacity and Eppendorf polypropylene pipette tips are being conducted. Results of these investigations will be presented elsewhere.

3.4 Conclusion

Second generation, TEOS-based coatings were realized on previously oxidized surfaces, introducing new chemical and topological properties, and applications to the material. Tubes coated with TEOS were relatively impermeable to toluene, introducing the idea that pre-glass coatings could be used to render polypropylene gas-impermeable. The idea is currently being tested using oxygen. A significant application made possible by the TEOS coating was the realization of mRNA purification. Initial steps in the patenting process for this method have been taken, as this method seems to be not only a convenient method for in-house production of surfaces for mRNA purification, but also could be feasible for industrial-scale production.

3.5 Acknowledgements

M.K. thanks Alpay Taralp and Zehra Sayers of Sabancı University for very helpful suggestions and assistance. In particular, M.K. wishes to thank Kivanç Bilecen of Sabancı University for assistance during the Total RNA isolation and mRNA purification.

3.6 References

- [1] A. S. D'Sonza, G. Pantano, *Mechanisms for Silanol Formation on Amorphous Silica Fracture Surfaces*, 100th annual Meeting of the American Chemical Society, Cincinnati, paper No. SXVII-003-97, 1998
- [2] R. K. Iler, *The Chemistry of Silica, Solubility, Polymerization, Colloid and Surface Properties, and Biochemistry*, John Wiley & Sons, 1979
- [3] Jun Lin et al., *Molecular Assembly in Orderes Mesoporosity: A New Class of Highly Functionalized Nanoscale Materials*, J. Phys. Chem. A, 104, 2000
- [4] D. Lin-Vien, N. B. Colthup, W. G. Fateley, J. G. Grasselli, *The Handbook of Infrared and Raman:Characteristic Frequencies of organic Molecules*, Academic Press, 1991
- [5] M. Hesse, H. Meier, B. Zeeh, *Organic Spectroscopy, Methods and Applications*, Thieme, Stuttgart, 1997
- [6] Pavia L. Donald, Gary M. Lampman, George S. Kriz, *Introduction to Spectroscopy: A Guide for Students of Organic Chemistry*, Harcourt Brace College Publishers, 2000
- [7] M. Peng, T. Kurokawa, J. P. Gong, Y. Osada, Q. Zheng, *Effect of surface roughness of hydrophobic substrate on heterogeneous polymerization of hydrogel.*, Journal of Physical Chemistry B, 106, 2002
- [8] E. P. Plueddemann, *Silane Coupling Agents*, Plenum Press, 1982
- [9] S. Thitinun, N. Thanabodeekij, A. M. Jamieson, S. Wongkasemjitt, *Sol-Gel Processing of Spirosilicates*, J. o. t. European Ceramic Society, 23 (3) 2000

Chapter 4: Second Generation Surfaces: Oxidized PP Coated Using TMPDT

4.1 Introduction

The results of the 2nd generation TEOS-coating experiments indicated that coatings can be used subsequently to increase the functionality of oxidized surfaces (Chapter 2).

Indeed, the results indicated that silanes can be used to coat oxidized surfaces in a convenient way using simple reaction procedures. The advantage of using silanes as coating materials is such that hundreds of different silanes are available and can be purchased from commercial suppliers. This fact offers immense possibilities for surface coatings affording different functional groups. To give some examples, surfaces bearing alcohol, amino, bromide, carboxylic acid, chloride, ester, ether groups in different aliphatic and aromatic variations can be produced easily using simple incubation methods. The surfaces afforded offer exceptional flexibility in life-science and chemistry applications, as the functional groups themselves may also serve as intermediates, allowing the formation of 3rd generation coatings using non-silane reagents. For example, silane-coated surfaces can be reacted with linker-reagents, affording protein-specific binding. Like other reactions discussed in this study, such modifications are very likely cost and time efficient and benefit of their ease.

While the TEOS method afforded a simple coating bearing surface pendant hydroxyl groups, further investigations were made to yield amino functionalized surfaces. The rationale for coating surface-pendant amino groups was to afford surfaces with the ability to bind proteins. For this purpose oxidized surfaces were coated with trimethoxysilylpropyldiethylenetriamine (TMPDT). Like other reactions in this study the coating method improved facility and cost efficiency, while the tube format featured easy handling.

4.2 Materials and Methods

Silanes, Chemicals, Proteins

Trimethoxysilylpropyldiethylenetriamine (TMPDT) was purchased from United Chemical Technologies (UCT) Inc. Ninhydrin (99%), bovine serum albumin (BSA) and 5-dimethylamino-1-naphthalenesulphonyl chloride (dansyl chloride) were obtained from Sigma-Aldrich Laborchemikalien GmbH. Glutaraldehyde was purchased from Merck KGaA. Dialysis bags (3500 molecular weight cut-off) were obtained from Pharmacia. Deionized water ($18\text{M}\Omega/\text{cm}^3$) was produced in-house using a Millipore Academic system. Reagent grade solvents were obtained from commercial suppliers.

4.2.1 General Methods (GM)

(i) Preparation of Aminosilane Solutions

Solutions of trimethoxysilylpropyldiethylene-triamine (TMPDT) of the composition organosilane/*i*-propanol (1:94) were prepared in Falcon Tubes (50ml). After the components were mixed using a VELP brand vortex, water (5%) was added to initiate the condensation reaction. This solution was incubated (15min, RT) affording the intermediate condensation products of TMPDT. TMPDT solutions were freshly prepared before each experiment to maintain consistency of the condensed products.

(ii) Washing and Drying of the Coated Surfaces

Following incubation, the reaction solutions were removed from the tubes using a pipette. Residing solutions were centrifuged using an Eppendorf brand micro-centrifuge (13200rpm, 1min) and subsequently removed. To wash the inner surfaces, the tubes were

filled with *i*-propanol. After withdrawing the washing solutions the tubes were dried *in vacuo* (70°C, 2h). To remove adsorbed but not immobilized reagent, as well as to assure the total hydrolysis of residual methoxysilanol bonds leading to maximum crosslinking of immobilized reagent, the tubes were once filled with water to the top. After the water was removed with the aid of a pipette, the tubes were dried again *in vacuo* (70°C, 2h).

(iii) Preparation and Ninhydrin Analyses of Coated surfaces

Ninhydrin solutions were prepared in Falcon Tubes (50ml) of the composition ninhydrin/*i*-propanol (99:1) using a VELP brand vortex and a Bandelin Ultrasonic Bath model SONOREX.

Accessible surface-pendant amino groups were verified by incubating the tubes (70°C, 40min) with ninhydrin solution (1%, 1.5ml). After the reaction, in which color was afforded, ninhydrin solutions were withdrawn and the tubes were washed extensively with water and dried (RT). Ninhydrin analyses were performed directly in the coated tubes. Ninhydrin solutions were freshly prepared before each experiment.

(iv) Preparation and Glutaraldehyde Analyses of Coated Surfaces

Aqueous glutaraldehyde solutions (5%) were prepared using falcon tubes (50ml) and a VELP brand vortex.

As with the ninhydrin analyses, no sample preparation was necessary. Reagent-accessible amino groups were crosslinked using these glutaraldehyde solutions (1.5ml, 40°C, 2h). Afterwards the reaction tubes were rinsed well with water and dried (RT). Glutaraldehyde solutions were freshly prepared before each experiment.

(v) Preparation and ATR-FTIR Analysis of Eppendorf Tubes

Eppendorf Tubes were prepared in a way that would permit effective analysis using the attenuated total reflectance (ATR) accessory of the FTIR instrument. As excessive bending of samples during the sample preparation yielded poor ATR-FTIR spectra, this modification to the method was introduced to protect the crystal structure of the polymer. A cylindrical piece with an approximate height of 3mm was cut from a region just above the hemispherical base of the tube using a razor blade heated in a Bunsen burner. The cylindrical ring was frozen in liquid nitrogen and shattered into small pieces with approximate dimensions of 2x3mm. These pieces were then *in vacuo* (40°C, 2h). Samples prepared in this way had little or no damage to the crystal structure but nevertheless some bore thick edges, which arose from the cutting action of the hot blade. These regions were carefully exercised with a flat-edged razor blade. The samples were tightly fixed over the measurement window of the ATR accessory of a Bruker model Equinox 55 infrared spectrophotometer. Twenty scans were averaged and displayed using rubber-band correction at 70 points in the Bruker OPUS V3.1 software of the system.

(vi) Trace Dansylation of Bovine Serum Albumin (BSA)

Heat-shock fractionated BSA (100mg) was dissolved in water (10ml) and the pH value was adjusted to 9 using sodium hydroxide solution (1M). 5-Dimethylamino-1-naphthalenesulfonyl chloride (Dansyl chloride, 5mg) was dissolved in acetonitrile (100µl) and slowly added to the gently stirring BSA solution maintaining the pH value between 8 and 9 using sodium hydroxide solution. After 1h, the solution was delivered into a dialysis bag and dialyzed (25°C) against 3x4L water. Ninhydrin color analysis of native albumin and dansylated albumin indicated that at most 10% of the amino groups had been transformed into the sulfonamide fluorophore. The dansylated protein was stored at 4°C.

(vii) Immobilization Method for Trace Dansylated Protein UV Analyses

A portion of the dansylated BSA stock was added to excess salt solution (1M NaCl) in order to afford a dilute stock (0.3mg protein/ml, pH 7) that would be appropriate for immobilization studies. This solution was transferred in the modified tubes and incubated (37°C, 1.5h). The solution was withdrawn, and the residing liquid was pooled by centrifugation and collected using a pipette. Photographs were obtained using an Uvitex UV-box with an Ihi CCD camera mounted. The tubes were filled with aqueous sodium chloride solution (1M, 1ml) and agitated (2min). The washing solution was withdrawn and the tubes were again photographed. Next, the tubes were washed with water and similarly documented. After that, the same washings were performed with 10% Triton X100 and 10% NP-40 solutions. Photographs were taken after every washing.

4.2.2 Second Generation TMPDT Coating Procedure

Previously oxidized Eppendorf Tubes were incubated (RT, 1.5h) with solutions of freshly prepared, half-condensed TMPDT (1.5ml). After reaction, the tubes were washed and dried as described previously (GM). TMPDT-coated samples were prepared using standard procedures (GM) and examined using ATR-FTIR methods.

Ninhydrin color analysis and glutaraldehyde-mediated surface transformations were performed directly after achieving the coating. Once more, visual and ATR-FTIR analyses were carried out after applying the standard sample preparation method for these analyses (GM). The protein binding performance of the aminated and glutaraldehyde-reacted tubes were investigated by incubating fluorescent BSA on these surfaces.

4.3 Results and Discussion

(i) TMPDT Coating

Previously oxidized surfaces, bearing carboxylic acid, ketone and hydroxyl groups, were coated with layers of TMPDT-silane during the performed experiments. The coating procedures were monitored using ATR-FTIR methods. The discussion is based on these spectral data and on basic organo-silane chemistry.

In the coating procedure, TMPDT can presumably bond to the oxidized surface by mainly four different reactions. One possible mode is that the aminosilanes bound to the surface in a manner similar to the coating with TEOS. A major difference between TMPDT and TEOS, however, is that the former contains amino groups and as such, the hydrolysis and condensation process is auto-catalytic. In a typical reaction, TMPDT should hydrolyze, hydrolysis-products of TMPDT dimerize, bind to the surface via hydrogen-bonding and these hydrogen-bonds finally condense to covalent bonds during the curing procedure [1-3].

Another possibility is that partially hydrolyzed silanol groups of TMPDT react directly with surface-pendant hydroxyl groups without dimerization (Figure 42) [1, 2].

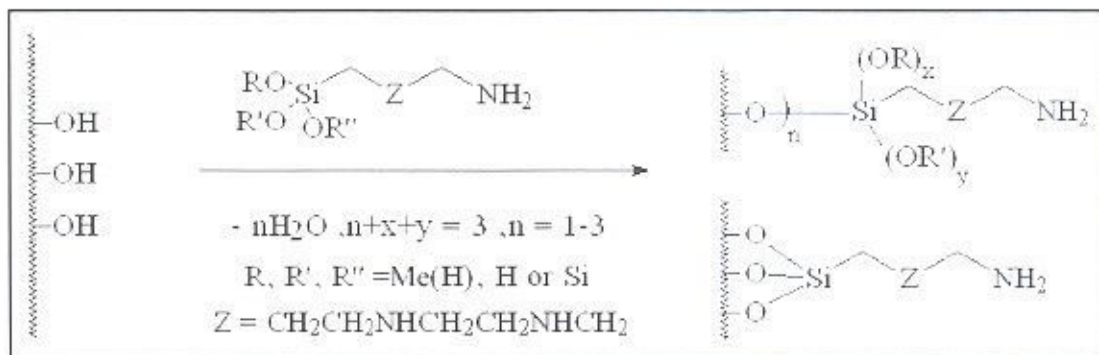


Figure 42: Reaction of TMPDT hydrolysis products and surface-pendant hydroxyl groups

Aside from the coating reactions initiated by the silanol-terminated ends of TMPDT, the aminosilane moieties could have also bonded to the surface, particularly at the amino-

terminated end. For example, the primary amino group of TMPDT could react with the carboxylic acid groups located on the oxidized surface, affording salt bridges (Figure 43) [3]. This mode of binding is also available to the two secondary amino groups. Primary

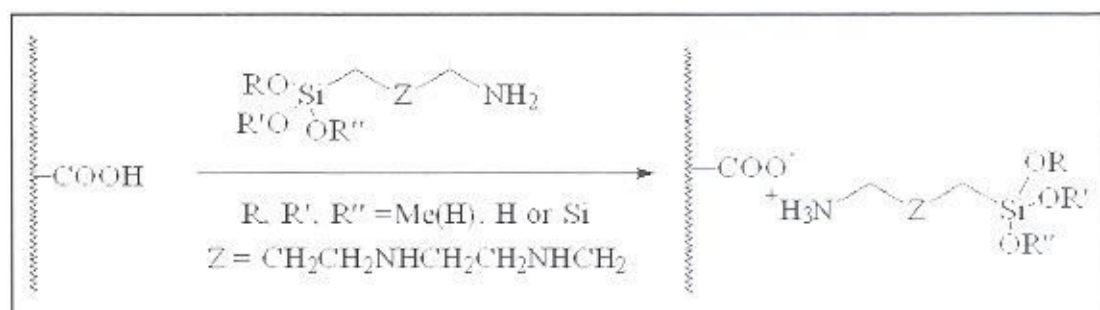


Figure 43: Reaction of TMPDT amino groups and surface-pendant carboxylic acids

amino groups of the TMPDT could also have anchored through the ketone groups located on the oxidized surfaces, affording imine bonds in the process (Figure 44) [3]. Both modes available to the amino groups in principle would leave the silane portion available for subsequent silane-silane self-condensation reactions. Reactions of secondary amino groups

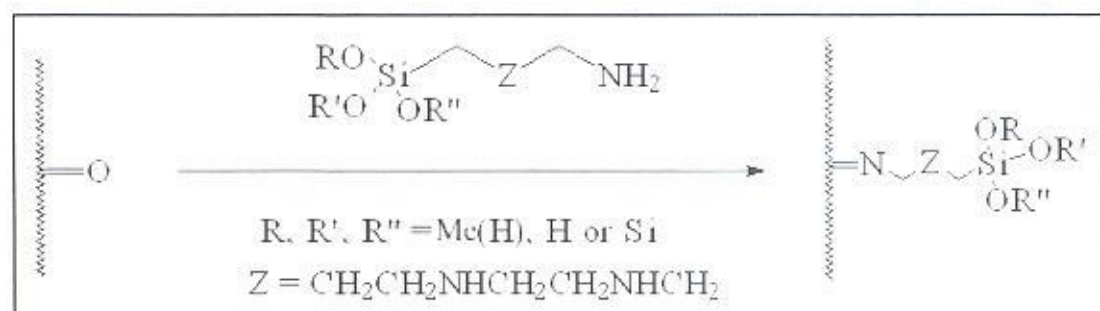


Figure 44: Reaction of TMPDT amino groups and surface-pendant ketones

of the TMPDT molecules with surface-pendant ketones to form encamines also seemed possible, but their potential contribution was not investigated further [3].

With due consideration to the possible modes of bonding, it follows that the coating afforded describes a complicated network of TMPDT surface adducts, self-condensates, and physisorbed groupings intertwined in the matrix of the polypropylene (Figure 45).

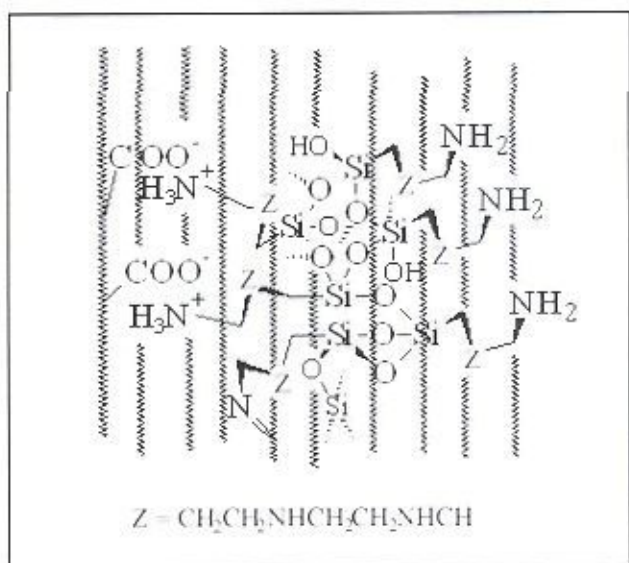


Figure 45: Model depicting the resultant coating of oxidized polypropylene by TMPDT

ATR-FTIR spectral data supported the discussed mechanism (Figure 46).

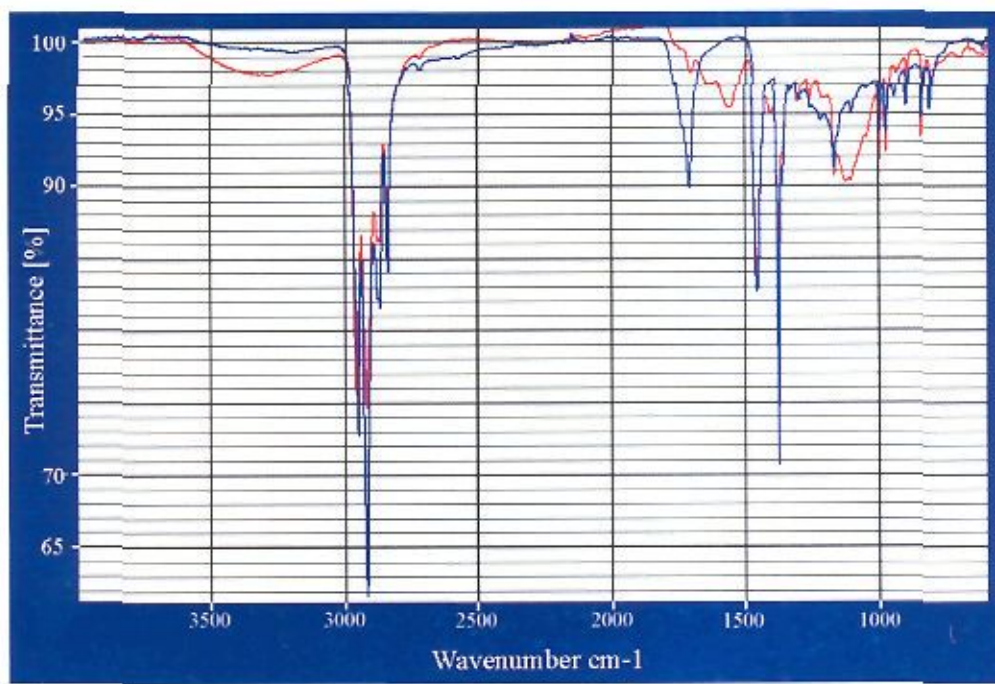


Figure 46: ATR-FTIR spectra of the oxidized (blue) and the TMPDT-coated (red) surfaces

Apparent imine formations were consistent with the results in that the intensity of carbonyl groups ($\nu_{C=O} = 1715\text{cm}^{-1}$) was reduced approximately by 80% following the reaction, implying that the accessible surface-pendant carbonyl groups were attacked by primary amino groups of the TMPDT. The condensation mechanisms were supported by the appearance of a strong N-H scissoring signal ($\nu_{N-H} = 1550\text{cm}^{-1}$) indicating the presence of immobilized free amino groups on the surface. Like the spectral data of the TEOS coating, the spectra of the TMPDT coating also afforded Si-O-C stretching frequencies ($\nu_{Si-O-C} = 1115\text{cm}^{-1}$) [4-6].

Ninhydrin tests validated the claim that TMPDT was successfully bound to the oxidized surfaces yet bore accessible amino groups [3]. In particular, ninhydrin-reacted tubes afforded significant violet-colored surfaces. No color change of the control surfaces could be noted during the ninhydrin reaction (Figure 47), consistent with the fact that amino groups were absent. Color in the tubes was permanently fixed, characteristic of

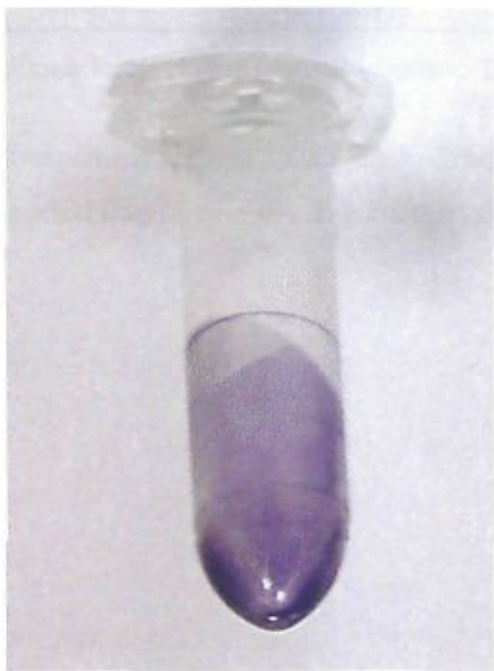


Figure 47: A TMPDT-coated tube followed ninhydrin reaction

entrapped chromophores from primary amino groups and covalently fixed chromophores originating from secondary amino groups. Quantitative ninhydrin analyses of the TMPDT-

coated tubes indicated that the loading of amino groups was approximately 200nmole/total cm².

(ii) Glutaraldehyde Crosslinking

Following the coating of TMPDT, free accessible amino groups were incubated with glutaraldehyde. Glutaraldehyde reacted by this procedure aldehyde groups bound to the TMPDT-coated surface (Figure 48) [7, 8]. Following reaction with glutaraldehyde,

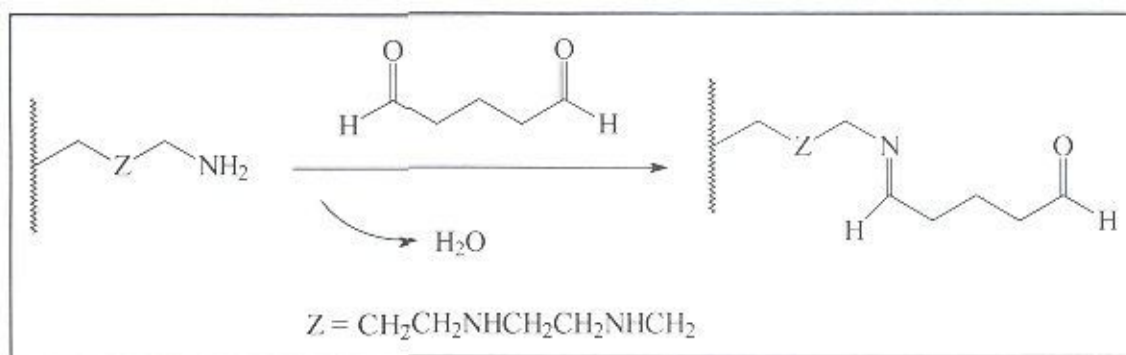


Figure 48: Reaction scheme for linking of glutaraldehyde to TMPDT-coated surfaces

tubes showed slightly yellow colored surfaces. Glutaraldehyde addition to the surface was validated by ATR-FTIR spectral data (Figure 49). In particular, spectroscopy indicated that

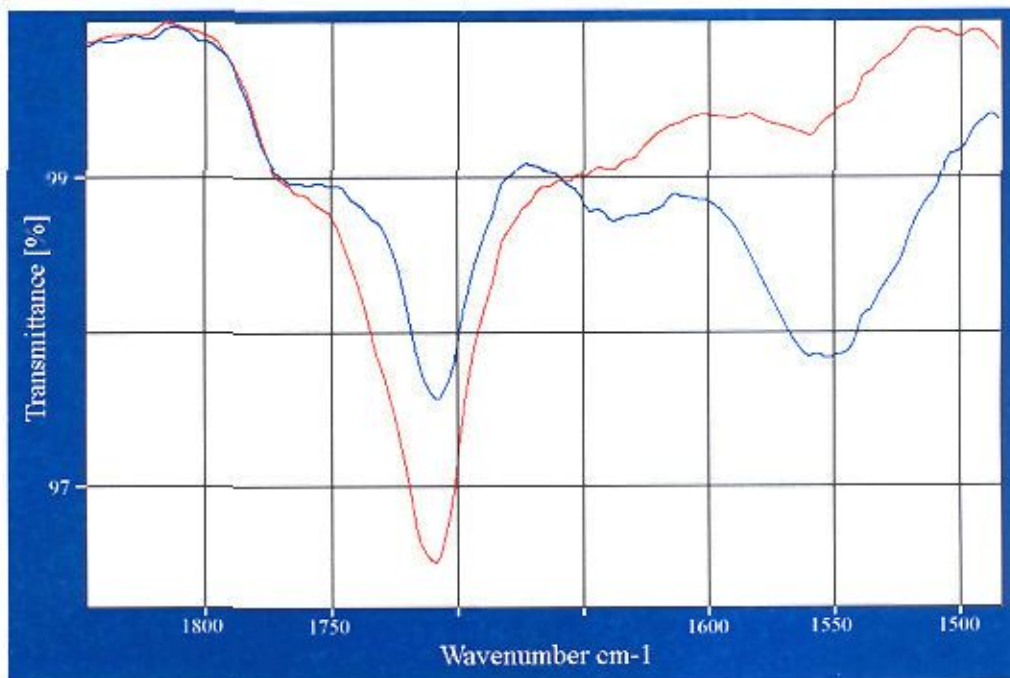


Figure 49: ATR-FTIR spectra of TMPDT-coated (blue) and glutaraldehyde adduct surfaces (red)

surface-pendant amino groups had reacted with glutaraldehyde solutions, as the N-H scissoring frequency ($\nu_{\text{N-H}} = 1550\text{cm}^{-1}$) was eliminated while the carbonyl stretching region ($\nu_{\text{C=O}} = 1720\text{-}1700\text{cm}^{-1}$) was increased [4 – 6, 9].

(iii) Protein Immobilization

Trace-dansylated BSA was immobilized onto TMPDT-coated surfaces as well as glutaraldehyde crosslinked TMPDT surfaces. UV-analyses that documented binding on TMPDT-coated surfaces pointed out, that protein was retained on the aminosilylated surfaces during the incubation protocol. Compared to TEOS-coated surfaces, TMPDT-coated surfaces retained protein in higher yield. This fact could be explained by the binding mechanisms of protein to the surfaces (Figure 50). While proteins bound to the TEOS surfaces mainly on the basis of hydrogen-bonding (A) and high surface area (B) TMPDT-coated surfaces allowed other modes of protein binding. Primary and secondary amines

located on the surface possible reacted with carboxylic acid groups of the protein affording salt bridges (C) [10, 11]. During the wash procedure, in which high salt solutions and water

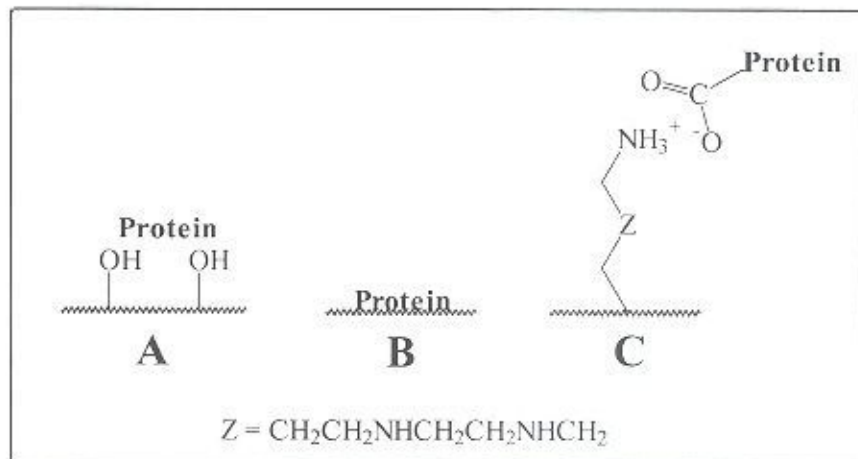


Figure 50: Protein binding schemes for TMPDT-coated surfaces

were used, the proteins were washed off the TMPDT-coated surfaces (not shown), attesting to the fact that proteins were bound by reversible interaction.

Glutaraldehyde-mediated TMPDT surfaces showed remarkably good performance in protein binding. In fact, protein was irreversibly bound to the glutaraldehyde-treated surfaces, presumably via imine formation between primary amino groups of the protein and the surface-pendant aldehyde groups (Figure 51:D) [3, 7, J]. In principle eneamines, formed

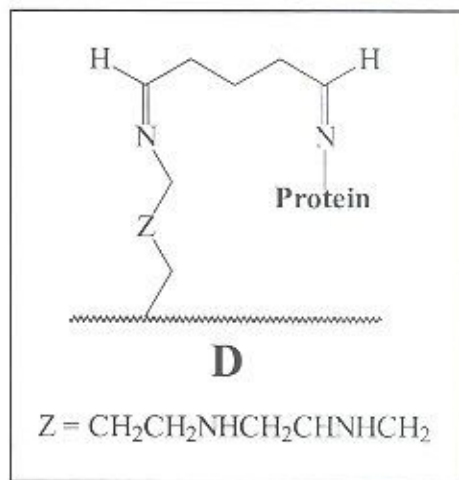


Figure 51: Protein binding schemes on glutaraldehyde-treated TMPDT surfaces

by the addition of secondary amino groups and surface-pendant aldehydes, may also have contributed to the irreversibility of the binding process [3].

In case of glutaraldehyde-treated TMPDT surfaces protein immobilization was not monitored by fluorescence, as previous experience showed that intercalated, unreacted glutaraldehyde could quench the fluorescence of dansylated BSA. The immobilization phenomena was analyzed using ATR-FTIR spectrometric methods. The obtained spectral data pointed out that protein, once retained by glutaraldehyde-crosslinking, could not be washed off by water or high salt solutions (Figure 52). In particular, spectral data validated

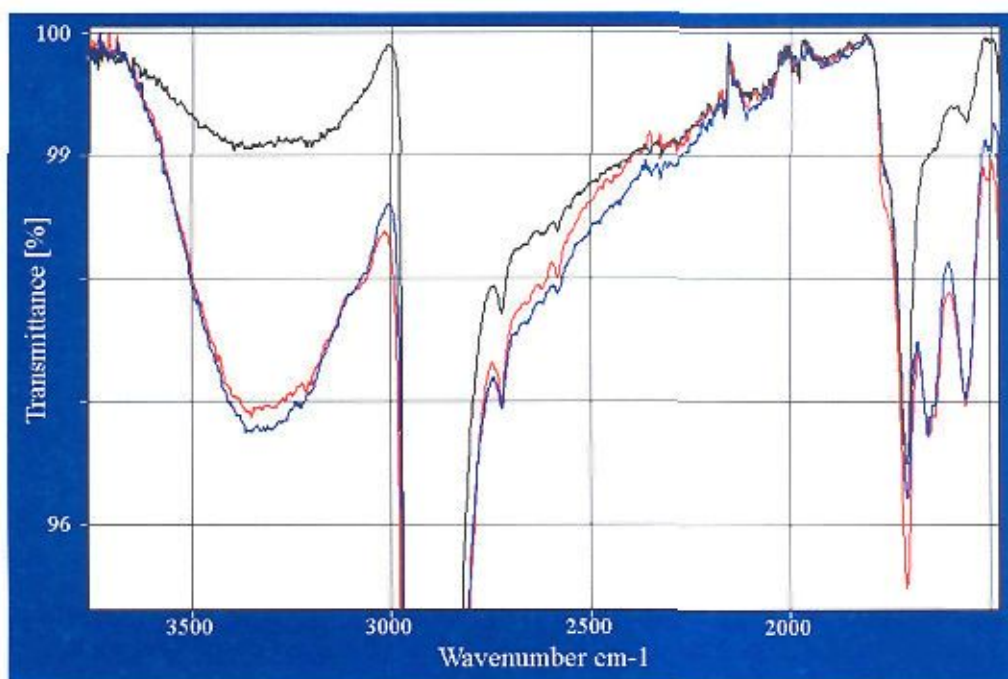


Figure 52: ATR-FTIR spectra of glutaraldehyde-treated surface before incubation with protein (black), after incubation with protein (blue), and following high salt washings (red).

the presence of protein, as signals in the N-H stretching range frequencies ($\nu_{N-H} > 3200\text{cm}^{-1}$) and the amide bond range ($\nu_{N-H} = 1600-1550\text{cm}^{-1}$) increased significant after protein was retained, while stretching signals in the aldehyde carbonyl region ($\nu_{C=O} = 1720-1700\text{cm}^{-1}$) decreased [4 – 6, 11]. Data obtained after the washing procedures showed no significant changes in the spectral profile. It follows that protein was permanently bound to the glutaraldehyde-treated TMPDT surfaces.

4.4 Conclusion

Oxidized surfaces were successfully coated with solutions of TMPDT to afford functionalized, reactive surfaces highly loaded with primary and secondary amino groups. The TMPDT-coated surfaces didn't retain immobilized proteins permanently, but offered possibilities for temporary protein adsorption. Linking of glutaraldehyde to TMPDT-coated surfaces afforded functionalized surfaces bearing aldehyde groups. With these surfaces, protein was irreversibly bound to the modified polypropylene tubes. The results indicated that glutaraldehyde-mediated TMPDT-coated surfaces showed possible potential for use as protein-carriers in biochemistry and life-science applications.

4.5 Acknowledgements

M.K. thanks Alpay Taralp of Sabancı University for very helpful suggestions and assistance.

4.6 References

- [1] A. S. D'Sonza, G. Pantano, *Mechanisms for Silanol Formation on Amorphous Silica Fracture Surfaces*, 100th annual Meeting of the American Chemical Society, Cincinnati, paper No. SXVII-003-97, 1998
- [2] R. K. Iler, *The Chemistry of Silica, Solubility, Polymerization, Colloid and Surface Properties, and Biochemistry*, John Wiley & Sons, 1979
- [3] J. March, *Advanced organic chemistry, 3rd edition*, John Wiley and Sons, 1985
- [4] D. Lin-Vien, N. B. Colthup, W. G. Fateley, J. G. Grasselli, *The Handbook of Infrared and Raman: Characteristic Frequencies of organic Molecules*, Academic Press, 1991
- [5] M. Hesse, H. Meier, B. Zeeh, *Organic Spectroscopy, Methods and Applications*, Thieme, Stuttgart, 1997
- [6] Pavia L. Donald, Gary M. Lampman, George S. Kriz, *Introduction to Spectroscopy: A Guide for Students of Organic Chemistry*, Harcourt Brace College Publishers, 2000
- [7] R. L. Lundblad, *Techniques in Protein Modification*, CRC Press, 1995
- [8] R. D. Frank, H. Dresbach, H. Thelm, H. G. Sieberth, *Glutaraldehyde Induces Fluorescence Technique (G.I.F.T): A New Method for the Imaging of Platelet Adhesion on Biomaterials*, J. o. Biomedical Materials Research, 52 (2), 2000
- [9] E. Scobbie, J. A. Groves, *An Investigation of the Composition of the Vapour Evolved Form Aqueous Glutaraldehyde Solutions*, Ann. Occup. Hyg., 39, 1995
- [10] J.-Y. Yoon, J.-H. Kim, W.-S. Kim, *Interpretation of protein adsorption phenomena onto functional microspheres*, Colloids and Surfaces B, 12, 1998
- [11] J.-H. Kim, J.-Y. Yoon, *Encyclopedia of Surface and Colloid Science*, 2002

General Conclusion

This investigation was based on the concept of using surface engineering to better integrate ordinary Eppendorf Safe-Lock Tubes in specialized areas of the life sciences. The results summarize that Eppendorf Tubes were modified easily to afford functionalized surfaces. The increase of surface area in particular was a significant development and merits continued investigation, as high-capacity plasticwares bearing functional groups will likely fulfill the needs of upcoming technologies. In this study, modified surfaces proved convenient to achieve mRNA purification and protein immobilization. Syntheses and analyses methods exemplified the ease by which researchers can customize and characterize their own surfaces. The prospect that a simple method can transform ordinary polypropylene tubes into convenience plastics for enzymic processing of substrates in analysis and synthesis laboratories should encourage continuing developments in this area. Modes of exploiting both the macroscopic and mesoscopic patterning are currently under investigation.

APPENDIX

I. Specifications of Analytical Equipment

(i) Attenuated Total Reflectance Infrared Spectrometer (FT)



Bruker EQUINOX 55
IR Spectrophotometer

Freq. Range: 7500-370 cm⁻¹
Beam splitter: multilayer coating on KBr
Detector: DTGS with KBr window
Inferometer: mechanical inferometer with
ROCKSOLID alignment
Additional equipment: DTGS, IR-ATR
(SensIR technologies), TGA-IR
Software: OPUS V3.1

(ii) X-Ray Powder Diffractometer



Bruker AXS D8 ADVANCE
X-ray Diffractometer

Measuring circles: 435, 500, 600mm
Angular range: 360°
Max usable angle range: -110° < 2Theta < 168°
Angular positioning: stepper motor with optical
encoders
Smallest step size: 0.0001°
Reproducibility: ± 0.0001°
Max. speed: 25°/sec
Software: DIFFRAC Plus 2.0

(iii) Differential Scanning Calorimeter (DSC)



NETZSCH DSC 204 Phoenix

Temp. range: -170 – 700°C

Reproducibility: < 0,1k

Sensitivity: 3-4,5 µV/mW

Combined with: TASC 414/4 system controller,
CC 200C cooling controller

Software: NETZSCH Measurement 4.1.1

II. Resume

Personal Information:

- Surname: Kolodzic
- Name: Markus
- Date of birth: 12.12.1977
- Place of birth: Munich
- Nationality: German
- Religion: Catholic

Home address:

Sudetenstr. 14A
82194 Gröbenzell
Germany

Education:

- 1989-1997 High school, "Gymnasium Gröbenzell",
82194 Gröbenzell
- 1997-2000 study of Chemistry, "Ludwig Maximilian
Universität", 80539 Munich
- Since 2000 study of Pharmaceutical Chemistry, Staatlich
anerkannte "Naturwissenschaftlich Technische Akademie",
NTA Prof. Dr. Grübler, 88316 Isny im Allgäu

Practical Experience :

- Student-laboratory experience: Organic and inorganic chemistry (qualitative, quantitative, synthesis), physical chemistry, biochemistry, microbiology, environmental chemistry, microscopy and physics
- Work experience:
 - ⇒ BSE-Test Laboratory, Pharmaceutical Laboratory,
88316 Isny im Allgäu, 2001-2002
 - ⇒ Research assistant (internship), Faculty of Engineering
and Natural Sciences, Sabancı University,
34956 Tuzla/Istanbul, 2002/2003